This is a revised version (previous manuscript Number. BLTN16-166)

Neoproterozoic-Cambrian petroleum system evolution of the Micang Shan Uplift, Northern Sichuan Basin, China: Insights from pyrobitumen Re-Os geochronology and apatite fission track analysis

Xiang Ge[1,2], Chuanbo Shen[1*], David Selby[2], Guozhi Wang[3], Zhao Yang[4], Yongjun Gong[1], Suofei Xiong[1]

[1]Key Laboratory of Tectonics and Petroleum Resources (China University of Geosciences), Ministry of Education, Wuhan, 430074, China

[2]Department of Earth Sciences, Durham University, Durham, DH1 3LE, UK

[3]Faculty of Earth Sciences, Chengdu University of Technology, Chengdu, 610059, China

[4]Department of Geology, Northwest University, Xi'an, 710069, China

[*]**Corresponding author: cugshen@126.com**

Acknowledgements

This work was supported by the National Natural Science Foundation of China (41672140, 41372140, 41273060, 41603042), the Program of Introducing Talents of Discipline to Universities (No. B14031), the Outstanding Youth Funding of Natural Science Foundation of Hubei Province (2016CFA055), the PetroChina Innovation Foundation (No. 2016D-5007-0103), the Fundamental Research Fund for the Central Universities (China University of Geosciences, CUG201536), the Wuhan Science and Technology Project (2016070204010145) and a China Scholarship Council (CSC) postgraduate award to Xiang Ge. David Selby acknowledges the TOTAL Endowment

Fund. We also thank Rachael Bullock, Barry J. Katz, Honghan Chen, Huaning Qiu, and two anonymous reviewers for their constructive comments.

Abstract

The Neoproterozoic strata of the Sichuan Basin is a key target for oil and gas. To evaluate the hydrocarbon evolution and its relationship with tectonic events in the Micang Shan Uplift, northernmost Sichuan Basin, we apply solid bitumen geochemistry (bitumen reflectance and fluorescence) and rhenium-osmium (Re-Os) geochronology.

The geochemistry of the solid bitumen indicates it is highly mature pyrobitumen that formed contemporaneously with dry gas generation during oil thermal cracking. The pyrobitumen is enriched in both Re (~106 - 191 ppb) and Os (~3030 - 5670 ppt). The Re-Os isotope data imply an Early Jurassic date for pyrobitumen formation, which coincides well with age estimates from fluid inclusion data and basin modelling. The Re-Os date for pyrobitumen formation coupled with previously presented AFT analysis show that exhumation of the Neoproterozoic strata occurred during the Cretaceous in the Micang Shan Uplift. This extensive uplift led to the erosion of any potential gas reservoirs and surface exposure of bitumen-bearing Neoproterozoic strata. In contrast, the more southern and central portions of the Sichuan Basin have experienced less severe exhumation and as result Neoproterozoic sourced gas systems are present. This study shows that through the combined application of Re-Os and AFT methodologies the timing of gas generation and subsequent erosion of any

potential gas reservoirs in the Micang Shan Uplift, northern Sichuan Basin can be quantified. Moreover, the Re-Os and AFT data illustrate the potential to constrain the timing of gas generation in petroleum systems worldwide.

Key words: Solid bitumen, Re-Os geochronology, Petroleum evolution, Gas generation, Sichuan Basin

1. Introduction

Hydrocarbon (oil and gas) production and shows sourced from or reservoired in Proterozoic to Cambrian successions occur worldwide, and are an important economic resource (Bhat et al., 2012; Craig et al., 2009; Ghori et al., 2009). For example, the Lena–Tunguska Proterozoic–Early Cambrian (microfossils and K-Ar dates on glauconites show the oldest date is 590 - 680 Ma) petroleum province, which includes the Lena Trough, the Kansk Basin, the Tunguska Basin, and the Sukhana Basin, located on the Siberian Craton, northern Russia, has a total estimated resource of 2 Bbbl (billion barrels) of oil and 83 Tcf (trillion cubic feet) of gas (Ghori et al., 2009; Meyerhoff, 1982). In addition, three potentially economically viable Proterozoic oil and gas systems have been found in Australia (McArthur, Urapungan and Centralian), which have a combined estimated resource of over 2 Bbbl of oil and 10 Tcf of gas (Bradshaw et al., 1994; Jackson et al., 1986; Munson, 2014). In the poorly explored Taoudenni Basin of North Africa, two deep exploration wells (Abolag-1 and Ouasa-1) have intersected a Neoproterozoic reservoir. A short duration open hole test on Abolag-1 well provided an estimated gas resource of 48000 scf (standard cubic feet) per day (Lottaroli et al., 2009). In China, the Sichuan Basin is another potentially prolific Proterozoic-Cambrian petroleum sourced area with an estimated resource of 26.2 Bbbl of oil and ~180 Tcf of gas (Fig. 1) (Ghori et al., 2009; Li et al., 2001; Zhang and Zhu, 2006; Zou et al., 2014a). Specific examples in the Sichuan Basin include the Weiyuan and Anyue gas fields, which are both sourced and reservoired in Neoproterozoic to Cambrian sedimentary rocks, and contain ~1.4 and ~15.4 Tcf of gas, respectively (Fig. 1) (Korsch et al., 1991; Li et al., 2015; Ma et al., 2010).

It is considered that much of the ‘‘easy exploration’’ around the world has been exhausted, and as a result industry is being forced to focus on more challenging exploration targets, such as Neoproterozoic-Cambrian strata (Bhat et al., 2012; Craig et al., 2009; Ghori et al., 2009). However, such systems typically possess significantly more complex geological evolution compared with conventional Phanerozoic petroleum systems, and as a result the exploration risk is greatly increased (Ghori et al., 2009; Katz and Everett, 2016). Further, as a direct outcome of multiple tectonic events, potential reservoirs have experienced high temperatures and pressures as well as uplift and subsidence. These factors, coupled with low quality seismic profiles, resulted in six decades of exploration to find the Anyue giant gas field following the discovery of the Weiyuan gas field in the Sichuan Basin (Wei et al., 2008; Zou et al., 2014a). Thus, in order to improve the exploration success rate of Proterozoic-Cambrian petroleum systems, a better understanding of their evolution, including timing of hydrocarbon generation, migration, accumulation and even trap destruction, is needed.

Basin modelling, as well as, hydrocarbon fluid inclusion analysis are widely used methods to constrain hydrocarbon evolution history (Angevine et al., 1990; Gonzaga et al., 2000; Parnell et al., 1996; Parnell et al., 2000; Schneider, 2003). However, imperfect kinetic models and poorly constrained parameters, such as the paleo-geothermal gradient, pressure and properties of the strata, hamper the accuracy of proposed evolution histories (Braun and Burnham, 1992; Roberts et al., 2004; Tissot et al., 1987). Since the 1980s, isotopic dating methods, for example, authigenic K-Ar illite (Dong et al., 1995; Lee et al., 1985; Meunier et al., 2004; Tohver et al., 2008), Ar-Ar K-feldspar (Mark et al., 2010), and Ar-Ar quartz fluid inclusion (Qiu et al., 2011), have all been shown to yield valuable information with regard to the timing of hydrocarbon generation and migration. However, authigenic illite K-Ar and Ar-Ar could only yield the maximum timing of hydrocarbon emplacement, given the challenge to isolate ^{40}Ar from samples (Dong et al., 1995; Mark et al., 2010). Additionally, Ar-Ar dating of quartz fluid inclusions requires samples to be enriched in gas-liquid inclusions. The latter, combined with the analytical challenge of isolating the Ar from the gas inclusions has limited the available results (Liu et al., 2011; Qiu et al., 2011). Compared to K-Ar and Ar-Ar dating on associated minerals, for example illite, K-feldspar and quartz fluid inclusions, rhenium-osmium (Re-Os) dating directly of the oil or solid bitumen, has shown promise to determine the absolute timing of hydrocarbon (oil and gas) generation (Cumming et al., 2014; Finlay et al., 2011; Ge et al., 2016; Georgiev et al., 2016; Lillis and Selby, 2013; Liu et al., 2017; Selby and

Creaser, 2005; Selby et al., 2005; Selby et al., 2007).

Solid bitumen can form at different evolutionary stages within a petroleum system (Jacob, 1989; Lewan, 1985; Meyer and De Witt Jr, 1990; Stasiuk, 1997; Wu et al., 2000). For example, asphalt and gilsonite are associated with crude oil generation, with impsonite and high maturity pyrobitumen considered to be related to crude oil decomposition or gas formation (Bernard et al., 2012; Lewan, 1997; Stasiuk, 1997; Wu et al., 2000; Xiao et al., 2007; Zhang and Li, 1999). To date, the available Re-Os data are for solid bitumen from the Polaris Mississippi Valley-type Zn-Pb deposit, Canada and the Northern Longmen Shan Thrust Belt, Southwest China, gilsonite from the Green River petroleum system in the Uinta Basin, western USA, and pyrobitumen from the Majiang-Wanshan reservoir, South China (Cumming et al., 2014; Ge et al., 2016; Ge et al., 2017; Selby et al., 2005).

The complex tectonic and hydrocarbon evolution of the Sichuan basin has resulted in highly debated timing and source models for many of hydrocarbon systems (e.g., the Weiyuan, Ziyang, Anyue and Puguang gas fields (Ma et al., 2007; Wei et al., 2008; Zhu et al., 2006)). Present research based on both structural and sedimentary analysis in the Sichuan basin suggests that the Late Silurian (ca. 420 Ma), Permian (ca. 250 Ma) and Early Jurassic (ca.180 Ma) could be key time intervals for both oil and gas generation (Li et al., 2016; Sun, 2008; Wang and Wang, 2011; Wang, 2015). Located in the north of the Sichuan Basin is the Micang Shan Uplift (Liu et al., 2015). Compared with the central or northwest Sichuan Basin, the Micang Shan Uplift has undergone additional tectonism since the Cretaceous (Chang et al., 2010; Sun et al., 2011a; Sun et al., 2011b; Yang et al., 2013) . Thrust tectonics during the Yanshan (ca. 150 Ma) or Himalayan orogeny (ca. 60Ma) resulted in the uplift of both Cambrian and Neoproterozoic strata to the surface (Dai et al., 2009).

Here we present solid bitumen Re-Os geochronology of the Micang Shan Uplift, coupled with bitumen reflectance, fluorescence analysis and previously published apatite fission track data (AFT age and thermal history modelling) to determine the Proterozoic-Cambrian hydrocarbon evolution process of the Micang Shan Uplift in the northern sector of the Sichuan Basin. Our data has potential implications for understanding the Proterozoic-Cambrian hydrocarbon evolution of other regions in the Sichuan Basin, and illustrates that the combined application of solid bitumen Re-Os geochronology and apatite fission track (AFT) analysis can provide valuable chronological data for petroleum evolution. In addition to Micang Shan Uplift, high maturity solid bitumen (pyrobitumen) occurs worldwide, e.g., in the Alberta Basin, Canada (Stasiuk, 1997), the Dahoney Basin, Nigeria (Meyer and De Witt Jr, 1990) and the Basque-Cantabrian Basin, Spain (Agirrezabala et al., 2008), this work are also potentially helpful for the hydrocarbon exploration worldwide.

2. Geological setting

The Micang Shan Uplift occurs along the northern margin of the Upper Yangtze block and comprises the northernmost sector of the Sichuan Basin, occupying an area of ~ 4500 km^2 (1737 mi^2) (Li et al., 2014). The Micang Shan Uplift is bordered by three different orogenic belts (Longmen Shan, Hannan Uplift, and the Daba Shan Orogeny), which lie to the west, northeast and east, respectively (Fig. 2) (Liu et al., 2015; Wang et al., 2014). From north to south, the Micang Shan Uplift is divided into three structural belts: the Basement Thrust Belt, the Submountain Fault-Fold Belt, and the South Foreslope (Huang, 2013). The entire Micang Shan Uplift records at least three orogenic events: 1) the Caledonian (ca. 480 Ma), 2) the Indosinian (ca. 200 Ma), and 3) the Yanshan (ca. 150 Ma) orogenies (Dong et al., 2012; Dong et al., 2011; Sun et al., 2011a; Sun et al., 2011b; Tian et al., 2012; Yang et al., 2013) (Fig. 3).

Structurally the Micang Shan Uplift represents a regional-scale anticline that comprises basement Neoproterozoic metavolcanics and granite, with overlying Neoproterozoic, Paleozoic (Cambrian to Silurian and Permian) and Mesozoic (Triassic and Jurassic) marine carbonate and clastic rocks (Qi et al., 2004; Wang et al., 2008) (Fig. 3). Solid bitumen is widely distributed within the Micang Shan Uplift in the Neoproterozic Dengying Formation (Dai et al., 2009). The Dengying Formation occurs over an area of 8500 km^2 (3281 mi^2), and has a maximum thickness of ~500 m (1640 ft), with an average thickness of ~100 m (328 ft). The estimated total solid bitumen reserves in the Dengying Formation of the Micang Shan Uplift and adjacent area is about 12.5 billion tons, which is equivalent to ~150 Bbbls of crude oil (Dai et al., 2009). The solid bitumen exists as pyrobitumen as a result of thermal cracking of pre-existing hydrocarbons (this study; see section 4 and 5 for details). Given the total abundance of pyrobitumen in the Micang Shan Uplift, the generated gas volume during pyrobitumen formation is determined to have exceeded 400 Tcf (Liu et al., 2015). As a result of tectonic uplift since the Cretaceous, all cap rocks in the Micang

Shan Uplift have been exhumed (Chang et al., 2010; Dai et al., 2010). In contrast, cap rocks are well developed in the more southern sectors of the Sichuan Basin. For example, the Cambrian and Silurian, and Triassic and Jurassic units are local seals in the Tongjiang and Bazhong regions (Liu et al., 2015). The Early Cambrian Qiongzhusi Formation is considered to be the principal source of the pyrobitumen in the Sichuan Basin, according to current biomarker analysis of the solid bitumen (though high maturity may affect the parameters) and potential source rocks (Liu et al., 2015; Zhang, 2013), element geochemistry evaluation of the potential sources (Cao et al., 2014) and the similar carbon isotope values of the Cambrian shale ($\delta^{13}C \sim 27.2$ ‰) and pyrobitumen ($\delta^{13}C \sim 27.5$ ‰).

3. Samples and methodology

The solid bitumen samples analysed in this study are representative of occurrences along the southern margin of the Micang Shan Uplift (Fig. 2). Solid bitumen occurs as accumulations as small as ~1 cm (0.39 in) long and ~ 0.2 - 0.5 cm (0.08 - 0.20 in) wide, and more commonly as ~ 3 - 5 cm (1.18 - 1.97 in) long and ~ 2 - 3 cm (0.79 - 1.18 in) wide (Fig. 4) within pores and fractures that are found widely distributed in the dolomite reservoir of the Dengying Formation. In hand specimens, the solid bitumen possesses a smooth and vitreous surface. Under the microscope, the bitumen is shown to occur intergrown with calcite and quartz, and to be predominantly hosted in hairline fractures or vugs. Eleven samples were collected from seven different locations. From east to west, these locations are the Jiulingzi(JLZ), Nanmushu(NMS), Mayuan(MY), Zhujiaba(ZJB), Kongxigou(KXG), Huitan(HT) and Yangba(YB) areas. The distance between each sample location is ~ 5 to 8 km (3 – 5 mi) (Fig. 2) (see Table 1 for latitude and longitude data). All the samples were collected from surface exposures and from similar stratigraphic levels within the Denying Formation, which dips at ~ 40° towards the southeast.

The solid bitumen fluorescence analyses were conducted at the Wuxi Institute of Petroleum Geology, SINOPEC. The solid bitumen-bearing limestones were first cut and polished into standard thin sections (~ 0.03 - 0.05 mm). The solid bitumen was examined using a Nikon ECLIPSE LV100N POL polarizing microscope under transmitted, reflected and fluorescent light at room temperature. The light source was a 100 W mercury lamp, with a digital photomicrography system. Bitumen reflectance (BRo, %) of incident light under oil immersion was used to assess the thermal maturity of samples. The reflectance microscope measures the amount of reflected light relative to the incident light and expresses this ratio as a percentage. The BRo value is obtained according to the formula, $BRo = (N - Ne)^2 + K^2 / (N + Ne)^2 + K^2$, where Ne is the refraction index of the oil used, N is the sample refraction, and K is the absorption coefficient (Zhang, 1988). The solid bitumen reflectance analyses were conducted at the Wuxi Institute of Petroleum Geology, SINOPEC, based on the method of (Zhang, 1988). The solid bitumen was first ground to ~ 0.15 mm, then mixed with resin and finally compressed into a cylindrical form. One surface of the cylinder was polished and immersed into oil with a refraction index (Ne) of 1.518. The sample refraction (N) was measured using a monochromatic light with a wavelength of 546 nm and a microscopy spectrophotometer (version: MPV-Ⅲ, 806(5)). The BRo value is determined through an average of 30 measured points in each sample.

The Re and Os isotopic analysis of the solid bitumen samples were analysed at the Laboratory for Source Rock and Sulfide Geochronology and Geochemistry (a member of the Durham Geochemistry Centre) at Durham University following published analytical procedures (e.g. Selby et al., 2005; Selby et al., 2007). Approximately 0.2 - 1.0 g bitumen was first separated from the limestone rocks without metal contact and crushed to ~ 1 mm grains using an agate pestle and mortar. Approximately 100 - 200 mg of bitumen were dissolved and equilibrated with a known amount of ^{185}Re and ^{190}Os spike solution by inverse *aqua-regia* (3 ml HCl and 6 ml HNO_3) in a Carius tube for 24 hours at 220˚C. Osmium was isolated and further purified from the inverse *aqua-regia* by $CHCl_3$ solvent extraction at room temperature and micro-distillation, respectively. The Re was isolated using HCl-HNO_3 based anion chromatography. The purified Re and Os were loaded on Ni and Pt filaments, respectively, and analyzed using Negative Ion Thermal Ionization Mass Spectrometry (N-TIMS). Rhenium was measured using Faraday collectors and Os in peak hopping mode using a secondary electron multiplier (SEM). Measured Re and Os ratios were corrected for oxide contribution and mass fractionation using $^{185}Re/^{187}Re = 0.59738$ (Gramlich et al., 1973) and $^{192}Os/^{188}Os = 3.08261$, spike and blank contributions. All data were blank corrected based on the total procedural blanks values of Re (1.6 ± 0.025 pg) and Os (0.05 ± 0.004 pg), with an average $^{187}Os/^{188}Os$ ratio of ~ 0.22 ± 0.06

(n = 4). All uncertainties include the propagated uncertainty in the standard, spike calibrations, mass spectrometry measurements, and blanks. The analyses presented in this study were conducted prior to using DROsS as the in-house control solution (Nowell et al., 2008) at Durham. The $^{187}Os/^{188}Os$ values of the Os standard solution AB2 during these studies were 0.1611 ± 0.0066, with the $^{185}Re/^{187}Re$ values of the Re standard solution being 0.5984 ± 0.0002. These values are in agreement with those previously published for AB2 and Re-std (Cumming et al., 2014; Finlay et al., 2011, 2012; Lillis and Selby, 2013; Rooney et al., 2012). The $^{185}Re/^{187}Re$ ratios for samples of this study were corrected for the measured difference of the $^{185}Re/^{187}Re$ value for Restd and the $^{185}Re/^{187}Re$ value of 0.59738 ± 0.00039 (Gramlich et al., 1973). The Re–Os data of this study are regressed using the program *Isoplot* V. 4.15 (Ludwig, 2008) using the ^{187}Re decay constant of $1.666\times10^{-11}a^{-1}$ (Smoliar et al., 1996). The input data contains $^{187}Re/^{188}Os$ and $^{187}Os/^{188}Os$ ratios with their total 2σ uncertainty and associated error correlation, Rho.

To further discuss the hydrocarbon and tectonic evolution of the Micang Shan Uplift, we have utilized the previously published Apatite Fission Track (AFT) data (n = 35) obtained from outcrop or borehole samples distributed over a north – south transect across the study area (Lei et al., 2012; Tian et al., 2012; Yang et al., 2013) (Fig. 2; Table. 2). In addition, thermal history modeling results (n = 15) in the study area are also utilized (Tian et al., 2012; Yang et al., 2013). These thermal history models are determined from eight Proterozoic granite, diorite or sandstone samples (MC01, MC02, MC25, NJ1T, NJ2T, NJ3T, NJ5T, NJ6T) located in the Micang Shan Uplift, and seven Paleozoic - Mesozoic sandstone samples (MC03, MC05, MC11, NJ12T, NJ15T, NJ17T, HB1-4) that are distributed in the southern area of the Micang Shan Uplift, e.g., the Submountain Fault-fold Belt and the South Foreslope (Fig. 2; Table 2).

4. Results

The bitumen reflectance (BRo, %), which is used in a similar way as vitrinite reflectance (Ro, %), is an indicator of thermal maturity of bitumen, and has become a tool used in basin analysis (Bertrand, 1993; Riediger, 1993). The BRo values become higher with increasing hydrocarbon maturity. According to the linear relationship between BRo and Ro (Jacob, 1989; Landis and Castaño, 1995; Schoenherr et al., 2007), bitumen at various maturity levels has different BRo values. For example, immature solid bitumen possess BRo values of < 0.25, with mature and over-mature solid bitumen being characterised by BRo values of ~ 1.1 and > 1.7 (Jacob, 1989; Landis and Castaño, 1995; Schoenherr et al., 2007). The BRo values of 3.25 to 4.08 (Table 1) for the five solid bitumen samples from the Micang Shan Uplift characterise the solid bitumen as thermally over-mature.

Ultraviolet fluorescence of the hydrocarbons (bitumen and oil) is also a useful tool for evaluating hydrocarbon maturity. With increasing maturity, the fluorescence color will gradually change from yellow-green, to brownish and finally to colorless (Chen, 2014; Jacob, 1989; Shi et al., 2015). The microscopic features of the solid bitumen samples (NMS and JLZ) from the Micang Shan Uplift are shown in Figure 5. The reservoir rocks are mainly composed of dolomite, containing pelletoid or granular-mosaic solid bitumen within fissures or between grains, with the solid bitumen possessing no fluorescence, thus characterizing the bitumen as highly mature (Fig. 5). Collectively, the organic petrography implies that the solid bitumen from the Micang Shan Uplift are pyrobitumen which formed through thermal cracking under high temperature environment, ≥ 140˚C (Dieckmann et al., 1998; Pepper and Corvi, 1995; Tsuzuki et al., 1999; Waples, 2000).

The Re and Os abundances of the solid bitumen samples range from ~ 106 to 191 ppb, and ~ 3030 to 5670 ppt, respectively (Table 1). These Re and Os abundances are significantly higher than those of average upper crustal values (Re = 0.198 ppb and Os = 31 ppt) (Esser and Turekian, 1993; Rudnick and Gao, 2003), but similar to values previously reported for bitumen and organic-rich sedimentary rocks (Cohen et al., 1999; Ge et al., 2016; Georgiev et al., 2016; Lillis and Selby, 2013; Ravizza and Turekian, 1992; Rooney et al., 2010; Xu et al., 2009a; Xu et al., 2014). The $^{187}Re/^{188}Os$ and $^{187}Os/^{188}Os$ values of the solid bitumen range from ~ 166 to 340, and ~ 2.82 to 3.74, respectively (Table 1). All the Re-Os data yield a Model 3 (assumes that the scatter about the best fit line is a combination of the assigned uncertainties and an unknown, but normally distributed variation in the $^{187}Os/^{188}Os$ values (Ludwig, 2008)) date of 239 ± 150 Ma (n = 11, Mean Squared Weighted Deviation (MSWD) = 398) (Fig. 6A), with an initial $^{187}Os/^{188}Os$ composition of 2.29 ± 0.64 (Table 1).

All the 35 AFT dates range from 123.5 ± 6.0 to 8.8 ± 1.3 Ma. The AFT dates are all younger than the intrusion or depositional ages of the sampled rocks, which indicate that the date represents the timing of thermal resetting. The AFT dates overall show a trend to younger dates from north to south across the Micang Shan Uplift into the Sichuan Basin (Fig. 2). The eleven samples in the Micang Shan Uplift possess older dates (~ 64 - 124 Ma) with a mean age of ca. 102 Ma. Eighteen outcrop samples from the inner Sichuan Basin possess AFT dates from ca. 60 to 83 Ma, with an average of ca. 70 Ma. The AFT dates from borehole HB1 from north Sichuan Basin (Fig. 2), with the exception of the most-shallow sample, HB1-4, which has a date of ca. 73 Ma, possess considerably younger dates (ca. 9 - 26 Ma). The mean track length of the thirty-five samples varies between 10.0 ± 0.45 and 13.23 ± 0.10 μm. Similar to the AFT date distribution, a decrease in track length is observed for samples from north to south (Table 2). The decreasing trend, in both AFT age and track length, from north to south implies variable cooling histories across the Sichuan Basin.

The thermal history (time-temperature path) could provide a more detailed understanding of the tectonic evolution of the Micang Shan Uplift and inner Sichuan Basin. Fifteen samples, six of our own remodelled samples (MC01, MC02, MC03, MC05, MC11, MC25) and nine previous published results (Tian et al., 2012) are shown here (Fig. 7). The thermal history are remodelled using the HeFTy software (version 1.8.4) based on the fanning curvilinear annealing model (Ketcham, 2005), c-axis projection (Donelick et al., 1999), and initial mean track length (L_0= 16.0 ± 0.8 μm) (Shen et al., 2012). For each sample, 100,000 to several million paths were calculated until at least 500 ‘good’ [T–t] paths were obtained (see (Yang et al., 2013) for the detailed modeling methodology). The thermal history modelling results of the fifteen samples can be divided into two groups. Group 1 comprise samples (n = 8) from the Micang Shan Uplift. Although there are some minor differences, cooling between ca. 140 and 100 Ma, with a temperature decrease from ~120 to 60 ºC (apatite partial annealing zone, APAZ) is revealed (Fig. 7). Group 2 comprise samples (n = 7) south of the study area and represent a cooling event between ca. 100 and 60 Ma, which implies that cooling to between ~120 and 60 ˚C in the more southern Sichuan Basin occurred ~40 myrs after that in the more northern Micang Shan Uplift (Fig. 7).

5. Discussion

5.1. Bitumen characteristics in the Micang Shan Uplift

Hydrocarbon evolution is a complex process that begins with diagenesis and the formation of the kerogen (Lewan, 1985; Tissot, 1984; Tissot and Welte, 1984). Solid bitumen, as a by-product of organic matter, exists through the entire hydrocarbon evolution process and records events such as hydrocarbon maturity, migration and accumulation pathways and the origin of the hydrocarbons (Wu et al., 2000). Processes, such as biodegradation, oxidation, phase-migration and thermal cracking, can lead to the formation of different types of solid bitumen (asphalt, gilsonite, grahamite, impsonite, anthroxolite, etc) (Jacob, 1989; Meyer and De Witt Jr, 1990; Rogers et al., 1974; Wu et al., 2000). The processes of oxidation, biodegradation, polymerization and devolatilization could result in the removal of the light hydrocarbons and form asphalt and gilsonite (Meyer and De Witt Jr, 1990). Phase-migration during hydrocarbon migration can lead to fluid differentiation through precipitation and de-asphalting (Meyer and De Witt Jr, 1990), resulting in the formation of grahamite, which typically occurs as veins (Stevenson et al., 1990; Zhang and Li, 1999). Thermal cracking, controlled by time and high temperature (Dahl et al., 1999; Vandenbroucke et al., 1999), of all hydrocarbons (e.g., oil, asphalt, gilsonite and grahamite) can result in the generation of dry gas and high maturity pyrobitumen (impsonite, antraxolite) (Meyer and De Witt Jr, 1990; Rogers et al., 1974).

High maturity pyrobitumen formed by thermal cracking is insoluble in most organic solvents and possesses different physical and chemical features compared with solid bitumen (Jacob, 1989; Mancuso et al., 1989; Rogers et al., 1974; Wu et al., 2000; Zhang and Li, 1999). For example, the solid bitumen types asphalt and gilsonite are characterized by low bitumen reflectance (BRo < 1.0%), high H/C atomic ratio (> 0.8), low Tmax (~ 450 ºC), and a yellow-green fluorescence colour. In contrast, the high maturity pyrobitumen types impsonite and anthroxolite possess high bitumen reflectance (BRo > 2.0 %), low H/C atomic ratio (< 0.6), high Tmax (~ 500 ºC), dark or no fluorescence, and contain high adamantine (3- + 4- methyl diamantane) concentrations (Fang et al., 2014; Hwang et al., 1998; Jacob, 1989; Shi et al., 2015; Wang et al., 2013; Yang et al., 2014).

All solid bitumen samples collected from the Micang Shan Uplift in this study have similar features (high bitumen reflectance (BRo = 3.25 – 4.08), no fluorescence and are insoluble in chloroform). Previous research in the Micang Shan Uplift area found that the bitumen was also characterized by high Tmax values (~ 540 ºC) (Huang, 2010). Collectively, the BRo values, fluorescence, Tmax, and lack of solubility in organic solvents characterise the solid bitumen in the Micang Shan Uplift as highly mature pyrobitumen. Although no gas reservoirs are known in the Micang Shan Uplift, the Neoproterozoic Weiyuan gas field in the Sichuan basin (Fig. 1), ~ 200 km (124 mi) south of the Micang Shan Uplift, possesses methane (CH_4) which comprises 85 % - 97 % of the total gas composition, with lesser amounts of nitrogen (N_2) (< 8%), carbon dioxide (CO_2) (< 5%) and ethane (C_2H_6)(< 1%) occupying the remaining components (Wei et al., 2008).

The molecular and isotope data (C_1-C_3 composition and $\delta^{13}C_1$- $\delta^{13}C_3$ value) are useful tools for identifying the gas formation mechanism (Behar et al., 1992; Prinzhofer and Huc, 1995). During thermal cracking, the $\ln(C_2/C_3)$ value will increase, but the $\ln(C_1/C_2)$ and the $\delta^{13}C_2$ - $\delta^{13}C_3$ values will remain the same for the generated gas (Prinzhofer and Huc, 1995). The gas from both the Ziyang and Weiyuan gas fields in the Western Sichuan Basin display $\ln(C_1/C_2)$ values within a narrow range (~5.5 - 7.0), but the $\ln(C_2 /C_3)$ ratio spans a much wider range (~1.0 - 6.5) (Liu et al., 2009). These data indicate that the gas was formed by thermal cracking of a previously formed reservoired oil. This also suggests that oils reservoired in the rest of the Sichuan Basin could have also experienced thermal cracking to form highly mature pyrobitumen and the accumulations of dry gas (CH_4) where trapped.

5.2. Timing of oil thermal cracking in the Micang Shan Uplift

Source rock hydrous pyrolysis experiments show that, initially, bitumen quantities increase as the amount of kerogen decreases, but as a result of increasing temperature, bitumen abundance decreases as it is cracked into liquid oil (Behar et al., 1991; Lewan, 1985). At higher temperatures (~ 360 ˚C), hydrous pyrolysis experiments show that the abundance of both bitumen and oil decrease in response to gas generation, as well as mass increasing in the source rock, which indicates the generation of high maturity pyrobitumen. The hydrous pyrolysis experiments indicate that the high maturity pyrobitumen and gas form contemporaneously during the last stages of hydrocarbon evolution. Further, recent studies on the thermal cracking of oil (Hill et al., 2003) and hydrocarbon composition numerical modelling (evolution of C_{14+} to C_1 compounds with time) in the Fahud Salt Basin, North Oman (Huc et al., 2000), found although pyrobitumen could form at the beginning of oil formation, the majority of the pyrobitumen formed together with the dry gas during the oil cracking event under high temperatures condition.

The Sichuan Basin contains more than 50 gas fields, which include the Ziyang, Weiyuan, Anyue and Puguang giant gas fields (Fig. 1) (Luo et al., 2013; Wei et al., 2008; Zou et al., 2014a). To date, there is still no agreement on the timing of the gas generation. Basin modelling of the Nanjiang area in the northern Sichuan Basin suggests that oil generation may have begun during the Late Cambrian to Ordovician (Wang and Wang, 2011). Following the exposure of the strata between the Devonian and Carboniferous, the entire Late Cambrian to Ordovician units of the Sichuan basin underwent rapid burial to ~7000 m (22,965 ft) between the Late Permian and Late Cretaceous (Fig. 8) (Liu et al., 2010; Ma et al., 2008; Wang and Wang, 2011).

Fluid inclusions can represent micron scale samples of the fluids (oil, gas and water) that flowed through and interacted with the host rocks during the evolution of a hydrocarbon system (Cooley et al., 2011; Haszeldine et al., 1984). Physical and chemical (pressure, temperature, fluid composition) conditions recorded by fluid inclusions within petroliferous basins have been widely applied to constrain both oil and gas migration and accumulation (Aplin et al., 1999; Bodnar, 1990; Bourdet et al., 2010; Cao et al., 2006; Oxtoby et al., 1995; Ping et al., 2017; Pironon, 2004; Teinturier et al., 2002). Fluid inclusion analysis in the Weiyuan Gas field, western Sichuan Basin, show that the homogenization temperatures of the aqueous fluid inclusions that are coeval with the gas-bearing fluid inclusions range from 108 - 212ºC, with an average of 158ºC (Tang et al., 2004). Furthermore, the fluid inclusion data from the Neoproterozic Dengying Formation reservoir in the Micang Shan Uplift possess homogenization temperatures that fall between 105 and 245 ºC, with 87% of the values being higher than 140 ºC and average temperature at 180 ºC (Fig. 8) (Wang, 2015). As to the few low temperature (< 120 ºC) data, it may relate to early hydrocarbon migration during the Silurian (Zou et al., 2014b) or the post-entrapment modification (Okubo, 2005). Applying the generally high homogenization temperatures to basin burial models within the northern Sichuan Basin (Liu et al., 2015; Sun, 2008; Yuan et al., 2012), a gas migration event is suggested to have occurred between the Triassic and Jurassic.

All the Re-Os data of the pyrobitumen from the Micang Shan Uplift area yield a date of 239 ± 150 Ma (n = 11, initial $^{187}Os/^{188}Os$ (Osi) = 2.29 ± 0.64, MSWD = 398). The

MWSD value obtained from the best-fit of all the Re-Os data suggests that the sample set have not fully met the criteria to obtain a precise isochron. For example, the entire sample set does not represent contemporaneous formation, or possess identical initial isotope compositions (Osi), or that the Re-Os systematics have been disturbed (Cohen et al., 1999; Kendall et al., 2009; Selby et al., 2007).

The percent deviation from the best-fit line of all the Re-Os data is illustrated in Figure 6B, which shows that samples HTB01, HTB02, JLZ4, YB01, KXG5 all show a large deviation (with the exception of sample KXG5 (~2.2%), > 4.4 %) from the best-fit line. Calculating the Osi value for each sample at 239 Ma (Osi_{239}), which is based on the Re-Os date of all eleven samples, shows that six samples (My601, My603, NMS955, NMS1030, NMS1068, ZJB01) possess very similar Osi_{239} values (2.25 - 2.30), with the remaining five samples (KXG05, HTB01, HTB02, YB01, JLZ04) possessing either slightly less or more radiogenic Osi values (1.96 - 2.15, n = 2; 2.36 - 2.52, n = 3, respectively) (Table 1). The differences in the Osi values may relate to samples bearing different initial Os isotope compositions or samples that represent different generation ages, or have experienced disturbance to the Re-Os isotope system. We discuss these possibilities below.

As stated above, the Re-Os data for the six samples with similar Osi values (My601, My603, NMS955, NMS1030, NMS1068, ZJB01, which are the samples that show the least deviation of the best-fit line of all the data, Fig. 6B) yield a Model 1 (which considers that only the assigned uncertainties produce the scatter about the best-fit line (Ludwig, 2008)) Re-Os date of 184 ± 23 Ma (Osi = 2.50 ± 0.09, MSWD = 1.0)

(Fig. 6C).

The remaining five samples plot in $^{187}Re/^{188}Os-^{187}Os/^{188}Os$ space either above or below the ca. 184 Ma isochron (Fig. 6C). Of these samples, sample KXG05 possesses an Osi_{239} value of 2.36, which falls between the Osi_{239} values for HTB01 and HTB02 (2.49 - 2.52), and JLZ04 and YB01 (1.96 - 2.15), and will therefore not fall along any best-fit line (Fig. 6C). Although the isochron dates determined from two samples are not considered a robust reflection of the true geologic age (Ludwig, 2008), we note that the Re-Os data for samples HTB01 and HTB02, and JLZ04 and YB01, yield Re-Os dates that are within uncertainty of the dates determined from the 6 samples (205 ± 32 Ma, Osi = 2.68 ± 0.16 and 173 ± 12 Ma, Osi = 2.34 ± 0.06, respectively (Fig. 6C)).

In the Micang Shan Uplift, the pyrobitumen may suffer from biodegradation, water washing during the migration and uplift process since formation. Previous work (Lillis and Selby, 2013; Selby and Creaser, 2005) found that the these effects do not appreciably disturb the Re-Os system. However, studies have found that the Re-Os system of the highly mature hydrocarbons, for example oil from Bighorn Basin, USA and bitumen from North Hebei Depression, China, may exhibit evidence of disturbance (Li et al., 2017; Lillis and Selby, 2013). Moreover, Re-Os isotope dating of pyrobitumen, which formed contemporaneously with dry gas, together with clastic AFT dating in the Majiang-Wanshan reservoir, South China show that the Re-Os date coincides with the timing related to gas generation and that the hydrocarbon thermal cracking event at temperatures of >140^{o} C could reset the previous oil or asphaltene

Re-Os system (Ge et al., 2016).

In this study, Latest Triassic to the Middle Jurassic dates (ca. 205 – 173 Ma) derived from the Re-Os pyrobitumen data, especially the ~184 Ma date determined from six samples, from the Micang Shan Uplift agree well with previous basin modelling (Yuan et al., 2012) and the general temporal understanding of oil and gas accumulation events in the northern Sichuan Basin (Liu et al., 2015). This age agreement indicates that the Late Triassic to Jurassic is the key period for thermally cracking of oil in Neoproterozoic reservoirs that resulted in gas generation and high maturity pyrobitumen (Fig. 8). Thus, although we cannot rule out disturbance to the Re-Os systematics of the pyrobitumen, the variation in the Osi values shown by the sample set most likely represents variations in the Os isotope composition of the petroleum that thermally cracked to produce pyrobitumen during the Late Triassic to the Middle Jurassic, and or the protracted interval over which pyrobitumen and gas generation occurred in the Michan Shan Uplift.

5.3. Petroleum system evolution of northern Sichuan Basin

Since the Late Triassic collision between the north China block and Yangtze block, which lead to the formation of the Qinling Orogeny (Yin and Nie, 1993), the Micang Shan Uplift was affected by a continuous compressional tectonic regime, with the most severe event occurring during the Cretaceous when the Yangtze block collided with Qinling Orogeny (south margin of the north China block) (Sun et al., 2011a; Sun et al., 2011b). During this tectonism the E-W trending fold and thrust structures between the Micang Shan Uplift and the inner Sichuan Basin were developed (Dong and Santosh, 2016; Xu et al., 2009b).

The Group 1 AFT samples from the Micang Shan Uplift have older AFT ages (ca. 64 - 124 Ma) with the thermal history modeling showing that the samples entered the apatite partial annealing zone (APAZ) between ca. 140 and 100 Ma, and cooled through the APAZ before ca. 90 Ma. In contrast, Group 2 samples, which are generally located at the transition zone between the Micang Shan Uplift and the inner Sichuan Basin, possess slightly younger ages (ca. 60 - 83 Ma) and thermal history modeling shows that the samples in this area pass in to the APAZ from ca. 100 to 60 Ma. The ~ 40 myr difference between both the AFT ages and the modeled cooling and uplift models coincide well with the N-S propagation of the tectonic front (Hu et al., 2012; Xu et al., 2009b). The AFT dates (ca. 60 to 124 Ma) and thermal history models indicate a prolonged and continuous cooling and uplift during the Cretaceous in the study area. Given the present-day thermal gradient (18 - 21ºC/km (Hu et al., 2000; Lu et al., 2005)) and the near surface temperature (~ 20ºC), more than 5000 m (16,404 ft) of strata is estimated to have been eroded as a result of the tectonic uplift during the Cretaceous. However, the much younger AFT dates (ca. 9 - 26 Ma) from the borehole HB1 (2594 – 4485 m (8510 – 14,714 ft) deep) in the Sichuan Basin (Table 2) indicate that the Cretaceous tectonic event did not affect the sediments within the inner Sichuan Basin, with the Jurassic and Triassic units currently at a depth of more than 2500 m (8202 ft). Moreover, many gas fields that are reservoired in the Neoproterozoic Dengying (Wei et al., 2008), Permian Changxing, and Triassic

Feixianguan formations (Ma et al., 2008) have been discovered within the central or southern Sichuan Basin (Fig. 1), which further prove that the tectonic event did not severely affect the inner Sichuan Basin. The presence of large quantities of pyrobitumen in the exposed and near-surface Neoproterozoic Dengying Formation and the absence of the Permian Changxing and Triassic Feixianguan formations in the northern Sichuan Basin (e.g., around the Micang Shan Uplift) suggest that ~ 5000 m (16,404 ft) of exhumation has occurred. Further evidence for uplift and erosion of the Proterozoic, Paleozoic and Mesozoic units of the Micang Shan Uplift is supported by a north-south paleocurrent direction (He et al., 1997; Meng et al., 2005), sandstone composition analysis (Dickinson et al., 1983; Liu et al., 2006), and detrital zircon U-Pb dates of the early Paleogene strata in the western Sichuan Basin (ca. 1800 – 130 Ma) (Jiang et al., 2013).

Integrating the pyrobitumen Re-Os data, AFT results (age and thermal history modeling) as well as previous basin models from the Micang Shan Uplift, permits the hydrocarbon evolution in the Micang Shan Uplift area to be quantitatively described as: (1) prior to the Caledonian Orogeny, Cambrian shales were buried to ~ 2500 m (8202 ft) depth throughout the whole Sichuan Basin and began to generate oil. However, subsequent uplift and exhumation during the Devonian to Carboniferous (Caledonian Orogeny) halted oil generation (Fig. 8a); (2) the Late Paleozoic-Early Mesozoic witnessed rapid sedimentation of the Permian to Triassic strata which resulted in the burial of the Neoproterozoic strata to ~ 7000 m (22,965 ft). Thermal cracking of the hydrocarbons under a high temperature environment (≥ 140 °C) as a result of burial the generation of pyrobitumen and dry gas occurred during the Late Triassic to Middle Jurassic (Fig. 8b); and (3) since the Cretaceous, related to the N-S compression between the north China block and Yangtze block, the Micang Shan Uplift experienced rapid uplift and exhumation, bringing the pyrobitumen-bearing Neoproterozoic strata to the surface and also resulted in the loss of the any gas-bearing reservoirs. In contrast, in the central and southern sectors of the Sichuan Basin, Paleozoic and Mesozoic gas reservoirs have been preserved due to limited uplift during the Late Cretaceous (Fig. 8c).

6. Conclusions and Implications

High maturity pyrobitumen Re-Os analysis, as well as previous basin modelling of the North Sichuan Basin, indicate that hydrocarbon thermal cracking (dry gas generation from oil cracking) in the northern Sichuan Basin occurred during the Early Jurassic (ca. 184 Ma), as a result of a high temperature environment due to rapid sedimentation and burial during the Late Permian to Jurassic in the Sichuan Basin. The AFT data (age and thermal history) indicate that the prolonged Cretaceous Yanshan Orogeny resulted in significant uplift and exhumation (~ 5000 m (16404 ft)) and caused the loss of Paleozoic and Mesozoic gas reservoirs in the Micang Shan Uplift, with only pyrobitumen remaining in the Neoproterozoic strata.

Previous work has shown that combined AFT and solid bitumen Re-Os geochronology on the Majiang-Wanshan reservoir, South China, has the potential to constrain the timing of oil cracking (pyrobitumen generation), and by inference, the timing of gas generation (Ge et al., 2016). Although the AFT and Re-Os dates were found to be similar in that work, the slightly older Re-Os date (ca. 80 Ma) compared to the AFT date (ca. 70 Ma) suggest that the temperature condition of resetting of the Re-Os systematics in hydrocarbons, specifically high maturity pyrobitumen, may be higher than that of the AFT closure temperature (110 ± 10 ºC) (Ge et al., 2016). Moreover, the Re-Os age derived from the pyrobitumen of the Micang Shan Uplift in this study is significantly older than the AFT dates, which further supports that the closure temperature of the Re-Os systematics in pyrobitumen is higher than that of the AFT closure temperature.

Deep burial and complex tectonic events have greatly affected the hydrocarbon systems in the Sichuan Basin, and even the whole of the south China block, resulting in gas being the main hydrocarbon resource (Zhao et al., 2004). The Re-Os data from this study imply that the gas in the Sichuan Basin formed during the Latest Triassic to the Middle Jurassic by thermal cracking. As such, the areas that have been relatively tectonically stable since the Mesozoic, e.g., in the ancient uplift or slope in the central and eastern Sichuan Basin (Zou et al., 2014a), may be prospective gas targets.

In addition to South China, pyrobitumen occurs worldwide, e.g., in the Alberta Basin, Canada (Stasiuk, 1997), the Dahoney Basin, Nigeria (Meyer and De Witt Jr, 1990) and the Basque-Cantabrian Basin, Spain (Agirrezabala et al., 2008). Thus, Re-Os pyrobitumen chronology (coupled with AFT dating) could be employed to yield quantitative timing of gas generation in other basins worldwide, and may enhance our understanding of the evolution of hydrocarbon systems and help guide gas exploration.

References cited

Agirrezabala, L. M., C. Dorronsoro, and A. Permanyer, 2008, Geochemical correlation of pyrobitumen fills with host mid-Cretaceous Black Flysch Group (Basque-Cantabrian Basin, western Pyrenees): Organic Geochemistry, v. 39, p. 1185-1188, doi: 10.1016/j.orggeochem.2008.03.012.

Angevine, C. L., P. L. Heller, and C. Paola, 1990, Quantitative sedimentary basin modeling, American Association of Petroleum Geologists, 139 p.

Aplin, A., G. Macleod, S. Larter, K. Pedersen, H. Sorensen, and T. Booth, 1999, Combined use of Confocal Laser Scanning Microscopyand PVT simulation for estimating the composition andphysical properties of petroleum in fluid inclusions: Marine and Petroleum Geology, v. 16, p. 97-110, doi: 10.1016/S0264-8172(98)00079-8.

Behar, F., S. Kressmann, J. L. Rudkiewicz, and M. Vandenbroucke, 1992, Experimental simulation in a confined system and kinetic modelling of kerogen and oil cracking: Organic Geochemistry, v. 19, p. 173-189, doi: 10.1016/0146-6380(92)90035-V.

Behar, F., P. Ungerer, S. Kressmann, and J. Rudkiewicz, 1991, Thermal evolution of crude oils in sedimentary basins: experimental simulation in a confined system and kinetic modeling: Oil & Gas Science and Technology, v. 46, p. 151-181, doi: 10.2516/ogst:1991007.

Bernard, S., R. Wirth, A. Schreiber, H.-M. Schulz, and B. Horsfield, 2012, Formation of nanoporous pyrobitumen residues during maturation of the Barnett Shale (Fort Worth Basin): International Journal of Coal Geology, v. 103, p. 3-11, doi: 10.1016/j.coal.2012.04.010.

Bertrand, R., 1993, Standardization of solid bitumen reflectance to vitrinite in some Paleozoic sequences of Canada: Energy Sources, v. 15, p. 269-287, doi: 10.1080/00908319308909027.

Bhat, G., J. Craig, M. Hafiz, N. Hakhoo, J. Thurow, B. Thusu, and A. Cozzi, 2012, Geology and hydrocarbon potential of Neoproterozoic–Cambrian Basins in Asia: an introduction: Geological Society, London, Special Publications, v. 366, p. 1-17, doi: 10.1144/SP366.15

Bodnar, R. J., 1990, Petroleum Migration in the Miocene Monterey Formation, California, USA: Constraints from Fluid-Inclusion Studies: Mineralogical Magazine, v. 54, p. 295-304, doi: 10.1180/minmag.1990.054.375.15.

Bourdet, J., J. Pironon, G. Levresse, and J. Tritlla, 2010, Petroleum accumulation and leakage in a deeply buried carbonate reservoir, Níspero field (Mexico): Marine and Petroleum Geology, v. 27, p. 126-142, doi: 10.1016/j.marpetgeo.2009.07.003.

Bradshaw, M., J. Bradshaw, A. Murray, D. Needham, L. Spencer, R. Summons, J. Wilmot, and S. Winn, 1994, Petroleum systems in West Australian basins: The Sedimentary Basins of Western Australia, Proceedings of the Petroleum Exploration Society of Australia Symposium, Perth, p. 93-118.

Braun, R. L., and A. K. Burnham, 1992, PMOD: a flexible model of oil and gas generation, cracking, and expulsion: Organic Geochemistry, v. 19, p. 161-172, doi: 10.1016/0146-6380(92)90034-U.

Cao, J., S. Yao, Z. Jin, W. Hu, Y. Zhang, X. Wang, Y. Zhang, and Y. Tang, 2006, Petroleum migration and mixing in the northwestern Junggar Basin (NW China): constraints from oil-bearing fluid inclusion analyses: Organic Geochemistry, v. 37, p. 827-846, doi: 10.1016/j.orggeochem.2006.02.003.

Cao, T., S. Xu, L. Zhou, and Y. Wang, 2014, Element Geochemistry Evaluation of Marine Source Rock with High Maturity: A Case Study of Lower Cambrian in Yangba Section of Nanjiang County, Sichuan: Earth Science-Journal of China University of Geosciences v. 39, p. 199-209, doi: 10.3799/dqkx.2014.019.

Chang, Y., C. Xu, W. R. Peter, and Z. Zhou, 2010, The exhumation evolution of the Micang Shang- Hanna Uplift since Cretaceous: Evidence form apatite (U-Th)/He dating: Chinese Journal of Geophysis, v. 53, p. 912-919, doi: 10.3969/j.issn.0001-5733.2010.04.016.

Chen, H., 2014, Microspectrofluorimetric characterization and thermal maturity assessment of individual oil inclusion: Acta Petrolei Sinica, v. 35, p. 584-590, doi: 10.7623/syxb201403023.

Cohen, A. S., A. L. Coe, J. M. Bartlett, and C. J. Hawkesworth, 1999, Precise Re–Os ages of organic-rich mudrocks and the Os isotope composition of Jurassic seawater: Earth and Planetary Science Letters, v. 167, p. 159-173, doi: 10.1016/S0012-821X(99)00026-6.

Cooley, M. A., R. A. Price, T. K. Kyser, and J. M. Dixon, 2011, Stable-isotope geochemistry of syntectonic veins in Paleozoic carbonate rocks in the Livingstone Range anticlinorium and their significance to the thermal and fluid evolution of the southern Canadian foreland thrust and fold belt: AAPG Bulletin, v. 95, p. 1851-1882, doi: 10.1306/01271107098.

Craig, J., J. Thurow, B. Thusu, A. Whitham, and Y. Abutarruma, 2009, Global Neoproterozoic petroleum systems: the emerging potential in North Africa: Geological Society, London, Special Publications, v. 326, p. 1-25, doi: 10.1144/SP326.1.

Cumming, V. M., D. Selby, P. G. Lillis, and M. D. Lewan, 2014, Re–Os geochronology and Os isotope fingerprinting of petroleum sourced from a Type I lacustrine kerogen: Insights from the natural Green River petroleum system in the Uinta Basin and hydrous pyrolysis experiments: Geochimica et Cosmochimica Acta, v. 138, p. 32-56, doi: 10.1016/j.gca.2014.04.016.

Dahl, J., J. Moldowan, K. Peters, G. Claypool, M. Rooney, G. Michael, M. Mello, and M. Kohnen, 1999, Diamondoid hydrocarbons as indicators of natural oil cracking: Nature, v. 399, p. 54-57, doi: 10.1038/19953.

Dai, H., S. Liu, W. Sun, K. Han, Z. Luo, Z. Xie, and Y. Huang, 2009, Study on Characteristics of Sinian-Silurian bitumen outcrops in the Longmesnshan - Micangshan area, Southwest China: Journal of Central South University (Science and Technology), v. 36, p. 687-696, doi: 10.3969/j.issn.1671-9727.2009.06.014.

Dai, H., S. Liu, W. Sun, Z. Zhang, and Y. Huang, 2010, Natural Gas Exploration Prospects of Simian System Dengying Formation in the Front Area of Micang Mountain: Journal of Southwest Petroleum University (Science & Technology Edition), v. 32, p. 16-26.

Dickinson, W. R., L. S. Beard, G. R. Brakenridge, J. L. Erjavec, R. C. Ferguson, K. F. Inman, R. A. Knepp, F. A. Lindberg, and P. T. Ryberg, 1983, Provenance of North American Phanerozoic sandstones in relation to tectonic setting: Geological Society of America Bulletin, v. 94, p. 222-235, doi: 10.1130/0016-7606(1983)94<222:PONAPS>2.0.CO;2.

Dieckmann, V., H. J. Schenk, B. Horsfield, and D. H. Welte, 1998, Kinetics of petroleum generation and cracking by programmed-temperature closed-system pyrolysis of Toarcian Shales: Fuel, v. 77, p. 23-31, doi: 10.1016/S0016-2361(97)00165-8.

Donelick, R. A., R. A. Ketcham, and W. D. Carlson, 1999, Variability of apatite fission-track annealing kinetics: II. Crystallographic orientation effects: American Mineralogist, v. 84, p. 1224-1234, doi: 10.2138/am-1999-0902.

Dong, H., C. M. Hall, D. R. Peacor, and A. N. Halliday, 1995, Mechanisms of argon retention in clays revealed by laser 40Ar-39Ar dating: Science, v. 267, p. 355-359, doi: 10.1126/science.267.5196.355.

Dong, Y., X. Liu, M. Santosh, Q. Chen, X. Zhang, W. Li, D. He, and G. Zhang, 2012, Neoproterozoic accretionary tectonics along the northwestern margin of the Yangtze Block, China: constraints from zircon U–Pb geochronology and geochemistry: Precambrian Research, v. 196, p. 247-274, doi: 10.1016/j.precamres.2011.12.007.

Dong, Y., and M. Santosh, 2016, Tectonic architecture and multiple orogeny of the Qinling Orogenic Belt, Central China: Gondwana Research, v. 29, p. 1-40, doi: 10.1016/j.gr.2015.06.009.

Dong, Y., G. Zhang, C. Hauzenberger, F. Neubauer, Z. Yang, and X. Liu, 2011, Palaeozoic tectonics and evolutionary history of the Qinling orogen: evidence from geochemistry and geochronology of ophiolite and related volcanic rocks: Lithos, v. 122, p. 39-56, doi: 10.1016/j.lithos.2010.11.011.

Esser, B. K., and K. K. Turekian, 1993, The osmium isotopic composition of the continental crust: Geochimica et Cosmochimica Acta, v. 57, p. 3093-3104, doi: 10.1016/0016-7037(93)90296-9.

Fang, Y., Y. Liao, L. Wu, and A. Geng, 2014, The origin of solid bitumen in the Honghuayuan Formation (O 1 h) of the Majiang paleo-reservoir—Evidence from catalytic hydropyrolysates: Organic Geochemistry, v. 68, p. 107-117, doi: 10.1016/j.orggeochem.2014.01.008.

Finlay, A. J., D. Selby, and M. J. Osborne, 2011, Re-Os geochronology and fingerprinting of United Kingdom Atlantic margin oil: Temporal implications for regional petroleum systems: Geology, v. 39, p. 475-478, doi: 10.1130/G31781.1.

Finlay, A. J., D. Selby, and M. J. Osborne, 2012, Petroleum source rock identification of United Kingdom Atlantic Margin oil fields and the Western Canadian Oil

Sands using Platinum, Palladium, Osmium and Rhenium: Implications for global petroleum systems: Earth and Planetary Science Letters, v. 313, p. 95-104, doi: 10.1016/j.epsl.2011.11.003.

Ge, X., C. Shen, D. Selby, D. Deng, and L. Mei, 2016, Apatite fission-track and Re-Os geochronology of the Xuefeng uplift, China: Temporal implications for dry gas associated hydrocarbon systems: Geology, v. 44, p. 491-494, doi: 10.1130/g37666.1.

Ge, X., C. Shen, D. Selby, J. Wang, L. Ma, X. Ruan, S. Hu, and L. Mei, 2017, Petroleum generation timing and source in the Northern Longmen Shan Thrust Belt, Southwest China: Implications for multiple oil generation episodes and sources: AAPG Bulletin, p. in press, doi: 10.1306/0711171623017125.

Georgiev, S. V., H. J. Stein, J. L. Hannah, R. Galimberti, M. Nali, G. Yang, and A. Zimmerman, 2016, Re–Os dating of maltenes and asphaltenes within single samples of crude oil: Geochimica et Cosmochimica Acta, v. 179, p. 53-75, doi: 10.1016/j.gca.2016.01.016.

Ghori, K., J. Craig, B. Thusu, S. Lüning, and M. Geiger, 2009, Global Infracambrian petroleum systems: a review: Geological Society, London, Special Publications, v. 326, p. 109-136, doi: 10.1144/SP326.6

Gonzaga, F., F. Gonalves, and L. Coutinho, 2000, Petroleum geology of the Amazonas Basin, Brazil: modeling of hydrocarbon generation and migration, in M. R. Mello and B. J. Katz, eds., Petroleum systems of South Atlantic margins, v. AAPG Memoir 73, p. 159-178.

Gramlich, J. W., T. J. Murphy, E. L. Garner, and W. R. Shields, 1973, Absolute Isotopic Abundance Ratio and Atomic Weight of a Reference Sample of Rhenium: Journal of reserch of the Notional Bureau of Standards - A. Physics and Chemistry, v. 77A, p. 691-698, doi: 10.6028/jres.094.034.

Haszeldine, R. S., I. M. S. Amp, and C. Cornford, 1984, Dating diagenesis in a petroleum basin, a new fluid inclusion method: Nature, v. 307, p. 354-357, doi: 10.1038/307354a0.

He, J., H. Lu, Q. Zhang, and B. Zhu, 1997, The Thrust Tectonic and Its Transpressive Geodynamics in Southern Dabashan Mountains: Geological Journal of China University v. 3, p. 419-428, doi: 10.16108/j.issn1006-7493.1997.04.009.

Hill, R. J., Y. Tang, and I. R. Kaplan, 2003, Insights into oil cracking based on laboratory experiments: Organic Geochemistry, v. 34, p. 1651-1672, doi: 10.1016/s0146-6380(03)00173-6.

Hu, J., H. Chen, H. Qu, G. Wu, J. Yang, and Z. Zhang, 2012, Mesozoic deformations of the Dabashan in the southern Qinling orogen, central China: Journal of Asian Earth Sciences, v. 47, p. 171-184, doi: 10.1016/2011.12.015.

Hu, S., L. He, and J. Wang, 2000, Heat flow in the continental area of China: a new data set: Earth and Planetary Science Letters, v. 179, p. 407-419, doi: 10.1016/S0012-821X(00)00126-6.

Huang, S., 2013, Study on the Muti-phase Fluid activities of Dengying Formation and tectonic uplift of Micang mountain area, Chengdu University of Technology, 71 p.

Huang, Y., 2010, Characteristics of Lower Palaeozoic Source Rocks in Micangshan Uplift Area, Sichuan Basin, Chengdu University of Technology, 77 p.

Huc, A. Y., P. Nederlof, R. Debarre, B. Carpentier, M. Boussafir, F. Laggoun-Défarge, A. Lenail-Chouteau, and N. Bordas-Le Floch, 2000, Pyrobitumen occurrence and formation in a Cambro–Ordovician sandstone reservoir, Fahud Salt Basin, North Oman: Chemical Geology, v. 168, p. 99-112, doi: 10.1016/S0009-2541(00)00190-X.

Hwang, R., S. Teerman, and R. Carlson, 1998, Geochemical comparison of reservoir solid bitumens with diverse origins: Organic Geochemistry, v. 29, p. 505-517, doi: 10.1016/S0146-6380(98)00078-3.

Jackson, M., T. Powell, R. Summons, and I. Sweet, 1986, Hydrocarbon shows and petroleum source rocks in sediments as old as 1.7× 109 years: Nature, v. 322, doi: 10.1038/322727a0.

Jacob, H., 1989, Classification, structure, genesis and practical importance of natural solid oil bitumen (“migrabitumen”): International Journal of Coal Geology, v. 11, p. 65-79, doi: 10.1016/0166-5162(89)90113-4.

Jiang, Z., H. Wu, X. Cui, J. Zhuo, and X. Jiang, 2013, Detrital Zircon U-Pb Geochronology of the Liujia Formation of the Paleogene in Sichuan Basin and its Geological Significance: Journal of Mineralogy and Petrology, v. 33, p. 76-84.

Katz, B. J., and M. A. Everett, 2016, An overview of pre-Devonian petroleum systems – Unique characteristics and elevated risks: Marine and Petroleum Geology, v.

73, p. 492-516, doi: 10.1016/j.marpetgeo.2016.03.019.

Kendall, B., R. A. Creaser, and D. Selby, 2009, 187Re-187Os geochronology of Precambrian organic-rich sedimentary rocks: Geological Society, London, Special Publications, v. 326, p. 85-107, doi: 10.1144/SP326.5.

Ketcham, R. A., 2005, Forward and inverse modeling of low-temperature thermochronometry data: Reviews in mineralogy and geochemistry, v. 58, p. 275-314, doi: 10.2138/rmg.2005.58.11.

Korsch, R., M. Huazhao, S. Zhaocai, and J. Gorter, 1991, The Sichuan basin, southwest China: a late proterozoic (Sinian) petroleum province: Precambrian Research, v. 54, p. 45-63, doi: 10.1016/0301-9268(91)90068-L.

Landis, C. R., and J. R. Castaño, 1995, Maturation and bulk chemical properties of a suite of solid hydrocarbons: Organic Geochemistry, v. 22, p. 137-149, doi: 10.1016/0146-6380(95)90013-6.

Lee, M., J. L. Aronson, and S. M. Savin, 1985, K/Ar dating of time of gas emplacement in Rotliegendes sandstone, Netherlands: AAPG Bulletin, v. 69, p. 1381-1385.

Lei, Y., C. Jia, B. Li, G. Wei, Z. Chen, and X. Shi, 2012, Meso‐Cenozoic tectonic events recorded by apatite fission track in the Northern Longmen‐Micang Mountains region: Acta Geologica Sinica (English edition), v. 86, p. 153-165.

Lewan, M., 1985, Evaluation of petroleum generation by hydrous pyrolysis experimentation: Philosophical Transactions of the Royal Society of London. Series A, Mathematical and Physical Sciences, v. 315, p. 123-134, doi:

10.1306/94886d71-1704-11d7-8645000102c1865d.

Lewan, M., 1997, Experiments on the role of water in petroleum formation: Geochimica et Cosmochimica Acta, v. 61, p. 3691-3723, doi: 10.1016/S0016-7037(97)00176-2.

Li, C., L. Wen, and S. Tao, 2015, Characteristics and enrichment factors of supergiant Lower Cambrian Longwangmiao gas reservoir in Anyue gas field: the oldest and largest single monoblock gas reservoir in China: Energy, Exploration & Exploitation, v. 33, p. 827-850, doi: 10.1260/0144-5987.33.6.827.

Li, F., Z. Shang, Z. Lou, Z. Zhu, M. Li, and X. Zhou, 2014, Geochemical characteristics of paleofluid and hydrocarbon preservation in marine strata of Micang-Daba piedmont and its adjacent.: Oil & Gas Geology, v. 35, p. 365-371, doi: 10.11743/ogg201410.

Li, J., Q. Cao, S. Lu, W. Wang, W. Li, X. Yan, Y. Shi, and J. yin, 2016, History of natural gas accumulation in Leshan-Longnyusi Sinian Paleo-uplit, Sichuan Basin: Oil & Gas Geology, v. 37, p. 30-36, doi: 10.11743/ogg2016020105.

Li, X., Z. Wang, X. Zhang, Q. Liu, and J. Yan, 2001, Charactersitics of Paleo-Uplifts in Sichuan Basin and their control on natural gases: Oil & Gas Geology, v. 22, p. 347-351.

Li, Z., X. Wang, K. Liu, S. Tessalina, X. Yang, X. Ma, and H. Sun, 2017, Rhenium-Osmium geochronology in dating petroleum systems: progress and chanllenges: Acta Petrolei Sinica, v. 38, p. 297-306, doi: 10.7623/syxb201703006.

Lillis, P. G., and D. Selby, 2013, Evaluation of the rhenium–osmium geochronometer in the Phosphoria petroleum system, Bighorn Basin of Wyoming and Montana, USA: Geochimica et Cosmochimica Acta, v. 118, p. 312-330, doi: 10.1016/j.gca.2013.04.01

Liu, J., D. Selby, M. Obermajer, and A. Mort, 2017, Re-Os geochronology and oil-source correlation of Duvernay Petroleum System, Western Canada Sedimentary Basin: Implications for the application of the Re-Os geochronometer to petroleum systems: AAPG Bulletin, p. in press

Liu, S., Y. Ma, X. Cai, G. Xu, G. Wang, Z. Yong, W. Sun, H. Yuan, and C. Pan, 2009, Characteristic and accumulation process of the natural gas from Sinian to Lower Paleozoic in Sichuan Basin, China: Journal of Central South University (Science and Technology), v. 36, p. 345-354.

Liu, S., Y. Ma, G. Wang, X. Cai, G. Xu, and W. Sun, 2015, Accumulation Process and Mechanism of the Palaeozoic Gas in the Sichuan Basin, Science Press, 440 p.

Liu, S., Z. Zhang, W. Huang, G. Wang, W. Sun, G. Xu, H. Yuan, C. Zhang, and B. Deng, 2010, Formation and destruction processes of upper Sinian oil-gas pools in the Dingshan-Lintanchang structural belt, southeast Sichuan Basin, China: Petroleum Science, v. 7, p. 289-301, doi: 10.1007/s12182-010-0071-3.

Liu, Y., Z. Guo, X. Liang, and Z. Yang, 2006, Tectonic Significance of Sandstones and Coupling relation of Basin and Mountain in the Late Triassic - Jurassic in the Middle and Upper Yangtze Region: Petroleum Geology & Experiment, v. 28, p. 201-205.

Liu, Z., L. Mei, H. Qiu, C. Shen, J. Tang, and J. Yun, 2011, 40Ar/39Ar geochronology constraints on hydrocarbon accumulation and destruction periods in the Bankeng paleo-reservoir in the southern margin of the middle Yangtze block: Chinese Science Bulletin, v. 56, p. 2803-2812, doi: 10.1007/s11434-011-4625-6.

Lottaroli, F., J. Craig, and B. Thusu, 2009, Neoproterozoic-Early Cambrian (Infracambrian) hydrocarbon prospectivity of North Africa: a synthesis: Geological Society, London, Special Publications, v. 326, p. 137-156, doi: 10.1144/SP326.7.

Lu, Q., S. Hu, and T. Guo, 2005, The background of the geothermal field for formation of abnormal high pressure in the northeastern Sichuan basin: Chinese Journal of Geophysics, v. 48, p. 1110-1116.

Ludwig, K., 2008, User's Manual for Isoplot 3.7: A geochronological toolkit for Microsoft Excel., v. Special Publication No.4: Berkeley Geochronological Centre, 76 p.

Luo, Z., J. Han, C. Luo, Q. Luo, and K. Han, 2013, The Discovery, Characteristics and Prospect of Commercial Oil and Gas Layers/Reservoirs in Sichuan Basin: Xinjiang Petroleum Geology, v. 34, p. 504-514.

Ma, Y., X. Cai, P. Zhao, Y. Luo, and X. Zhang, 2010, Distribution and futher exploration of the Large-medium sized gas field in Sichuan Basin: Acta Geologica Sinica, v. 31, p. 347-354.

Ma, Y., X. Guo, T. Guo, R. Huang, X. Cai, and G. Li, 2007, The Puguang gas field:

New giant discovery in the mature Sichuan Basin, southwest China: AAPG Bulletin, v. 91, p. 627-643, doi: 10.1306/11030606062.

Ma, Y., S. Zhang, T. Guo, G. Zhu, X. Cai, and M. Li, 2008, Petroleum geology of the Puguang sour gas field in the Sichuan Basin, SW China: Marine and Petroleum Geology, v. 25, p. 357-370, doi: 10.1016/j.marpetgeo.2008.01.010.

Mancuso, J. J., W. A. Kneller, and J. C. Quick, 1989, Precambrian vein pyrobitumen: evidence for petroleum generation and migration 2 Ga ago: Precambrian research, v. 44, p. 137-146, doi: 10.1016/0301-9268(89)90079-X.

Mark, D. F., J. Parnell, S. P. Kelley, M. R. Lee, and S. C. Sherlock, 2010, 40Ar/39Ar dating of oil generation and migration at complex continental margins: Geology, v. 38, p. 75-78, doi: 10.1130/G30237.1.

Meng, Q. R., E. Wang, and J. M. Hu, 2005, Mesozoic sedimentary evolution of the northwest Sichuan basin: Implication for continued clockwise rotation of the South China block: Geological Society of America Bulletin, v. 117, p. 396-410, doi: 10.1130/B25407.1.

Meunier, A., B. Velde, and P. Zalba, 2004, Illite K–Ar dating and crystal growth processes in diagenetic environments: a critical review: Terra Nova, v. 16, p. 296-304, doi: 10.1111/j.1365-3121.2004.00563.x.

Meyer, R. F., and W. De Witt Jr, 1990, Definition and world resources of natural bitumens, United States Department of the Interior, United States Geological Survey, 14 p.

Meyerhoff, A. A., 1982, Hydrocarbon resources in arctic and subarctic regions: CSPG

Special Publications p. 451-552, doi: 10.1016/0165-232x(83)90063-0.

Munson, T., 2014, Petroleum geology and potential of the onshore Northern Territory, 2014: Northern Territory Geological Survey, Report, v. 22, p. 252.

Nowell, G., D. Pearson, S. Parman, A. Luguet, and E. Hanski, 2008, Precise and accurate 186Os/188Os and 187Os/188Os measurements by multi-collector plasma ionisation mass spectrometry, part II: Laser ablation and its application to single-grain Pt–Os and Re–Os geochronology: Chemical Geology, v. 248, p. 394-426, doi: 10.1016/j.chemgeo.2007.12.004.

Okubo, S., 2005, Effects of thermal cracking of hydrocarbons on the homogenization temperature of fluid inclusions from the Niigata oil and gas fields, Japan: Applied Geochemistry, v. 20, p. 255-260, doi: 10.1016/j.apgeochem.2004.09.001.

Oxtoby, N. H., A. W. Mitchell, and J. G. Gluyas, 1995, The filling and emptying of the Ula Oilfield: fluid inclusion constraints: Geological Society Special Publications, v. 86, p. 141-157, doi: 10.1144/GSL.SP.1995.086.01.11.

Parnell, J., P. Carey, and B. Monson, 1996, Fluid inclusion constraints on temperatures of petroleum migration from authigenic quartz in bitumen veins: Chemical geology, v. 129, p. 217-226, doi: 10.1016/0009-2541(95)00141-7.

Parnell, J., C. Honghan, D. Middleton, T. Haggan, and P. Carey, 2000, Significance of fibrous mineral veins in hydrocarbon migration: fluid inclusion studies: Journal of Geochemical Exploration, v. 69-70, p. 623-627, doi: 10.1016/S0375-6742(00)00040-6.

Pepper, A. S., and P. J. Corvi, 1995, Simple kinetic models of petroleum formation. Part I: oil and gas generation from kerogen: Marine and Petroleum Geology, v. 12, p. 291-319, doi: 10.1016/0264-8172(95)98381-E.

Ping, H., H. Chen, and G. Jia, 2017, Petroleum accumulation in the deeply buried reservoirs in the northern Dongying Depression, Bohai Bay Basin, China: New insights from fluid inclusions, natural gas geochemistry, and 1-D basin modeling: Marine and Petroleum Geology, v. 80, p. 70-93, doi: 10.1016/j.marpetgeo.2016.11.023.

Pironon, J., 2004, Fluid inclusions in petroleum environments: analytical procedure for PTX reconstruction: Acta Petrolei Sinica, v. 20, p. 1332-1342.

Prinzhofer, A. A., and A. Y. Huc, 1995, Genetic and post-genetic molecular and isotopic fractionations in natural gases: Chemical Geology, v. 126, p. 281-290, doi: 10.1016/0009-2541(95)00123-9.

Qi, W., M. Hou, K. Wang, Z. Yang, and D. wang, 2004, A large-scale stratabound lead-zinc metallogenic belt discoved in the Mayuan area, Nanzheng County, Shanxi: Geological Bulletin of China, v. 23, p. 1139-1142.

Qiu, H.-N., H.-Y. Wu, J.-B. Yun, Z.-H. Feng, Y.-G. Xu, L.-F. Mei, and J. Wijbrans, 2011, High-precision 40Ar/39Ar age of the gas emplacement into the Songliao Basin: Geology, v. 39, p. 451-454, doi: 10.1130/G31885.1.

Ravizza, G., and K. Turekian, 1992, The osmium isotopic composition of organic-rich marine sediments: Earth and Planetary Science Letters, v. 110, p. 1-6, doi: 10.1016/0012-821X(92)90034-S.

Riediger, C., 1993, Solid bitumen reflectance and Rock-Eval T max as maturation indices: an example from the “Nordegg Member”, Western Canada Sedimentary Basin: International Journal of Coal Geology, v. 22, p. 295-315, doi: 10.1016/0166-5162(93)90031-5.

Roberts, L. N., M. D. Lewan, and T. M. Finn, 2004, Timing of oil and gas generation of petroleum systems in the Southwestern Wyoming Province: Mountain Geologist, p. 87-117.

Rogers, M., J. McAlary, and N. Bailey, 1974, Significance of reservoir bitumens to thermal-maturation studies, Western Canada Basin: AAPG Bulletin, v. 58, p. 1806-1824, doi: 10.1306/83d919b6-16c7-11d7-8645000102c1865d.

Rooney, A. D., D. Selby, J.-P. Houzay, and P. R. Renne, 2010, Re–Os geochronology of a Mesoproterozoic sedimentary succession, Taoudeni basin, Mauritania: implications for basin-wide correlations and Re–Os organic-rich sediments systematics: Earth and Planetary Science Letters, v. 289, p. 486-496, doi: 10.1016/j.epsl.2009.11.039.

Rooney, A. D., D. Selby, M. D. Lewan, P. G. Lillis, and J.-P. Houzay, 2012, Evaluating Re–Os systematics in organic-rich sedimentary rocks in response to petroleum generation using hydrous pyrolysis experiments: Geochimica et Cosmochimica Acta, v. 77, p. 275-291, doi: 10.1016/j.gca.2011.11.006.

Rudnick, R., and S. Gao, 2003, Composition of the continental crust: Treatise on geochemistry, v. 3, p. 1-64, doi: 10.1016/0016-7037(95)00038-2.

Schneider, F., 2003, Basin modeling in complex area: examples from Eastern

Venezuelan and Canadian Foothills: Oil & gas science and technology, v. 58, p. 313-324, doi: 10.2516/ogst:2003019.

Schoenherr, J., R. Littke, J. L. Urai, P. A. Kukla, and Z. Rawahi, 2007, Polyphase thermal evolution in the Infra-Cambrian Ara Group (South Oman Salt Basin) as deduced by maturity of solid reservoir bitumen: Organic Geochemistry, v. 38, p. 1293-1318, doi: 10.1016/j.orggeochem.2007.03.010.

Selby, D., and R. A. Creaser, 2005, Direct radiometric dating of hydrocarbon deposits using rhenium-osmium isotopes: Science, v. 308, p. 1293-1295, doi: 10.1126/science.1111081.

Selby, D., R. A. Creaser, K. Dewing, and M. Fowler, 2005, Evaluation of bitumen as a 187Re–187Os geochronometer for hydrocarbon maturation and migration: a test case from the Polaris MVT deposit, Canada: Earth and Planetary Science Letters, v. 235, p. 1-15, doi: 10.1016/j.epsl.2005.02.018.

Selby, D., R. A. Creaser, and M. G. Fowler, 2007, Re–Os elemental and isotopic systematics in crude oils: Geochimica et Cosmochimica Acta, v. 71, p. 378-386, doi: 10.1016/j.gca.2006.09.005.

Shen, C.-B., R. A. Donelick, P. B. O'Sullivan, R. Jonckheere, Z. Yang, Z.-B. She, X.-L. Miu, and X. Ge, 2012, Provenance and hinterland exhumation from LA-ICP-MS zircon U–Pb and fission-track double dating of Cretaceous sediments in the Jianghan Basin, Yangtze block, central China: Sedimentary Geology, v. 281, p. 194-207, doi: 10.1016/j.sedgeo.2012.09.009.

Shi, C., J. Cao, J. Bao, C. Zhu, X. Jiang, and M. Wu, 2015, Source characterization of highly mature pyrobitumens using trace and rare earth element geochemistry: Sinian–Paleozoic paleo-oil reservoirs in South China: Organic Geochemistry, v. 83-84, p. 77-93, doi: 10.1016/j.orggeochem.2015.03.008.

Smoliar, M. I., R. J. Walker, and J. W. Morgan, 1996, Re-Os ages of group IIA, IIIA, IVA, and IVB iron meteorites: Science, v. 271, p. 1099-1102, doi: 10.1126/science.271.5252.1099.

Stasiuk, L. D., 1997, The origin of pyrobitumens in Upper Devonian Leduc Formation gas reservoirs, Alberta, Canada: an optical and EDS study of oil to gas transformation: Marine and Petroleum Geology, v. 14, p. 915-929, doi: 10.1016/S0264-8172(97)00031-7.

Stevenson, J., J. Mancuso, J. Frizado, P. Truskoski, and W. Kneller, 1990, Solid pyrobitumen in veins, Panel Mine, Elliot Lake District, Ontario: Canadian Mineralogist, v. 28, p. 161-169.

Sun, D., S. Liu, B. Deng, Z. Li, Y. Zhong, Y. Huang, and Z. Xie, 2011a, Superposed fold characteristics and structural evolution in the junction area of Longmenshan Mountains and Micangshan Mountains in the southwest of China Journal of Chengdu University of Technology (Science & Technology Edition), v. 38, p. 156-168.

Sun, D., S. Liu, Z. Li, W. Sun, B. Deng, Y. Zhong, and J. Li, 2011b, The characteristic and transfer model of Micang Mountain structural transfer zone: Chinese Journal of Geology, v. 46, p. 620-637.

Sun, W., 2008, The Research of the Formation Process and Mechanism of Gas Pools in Proterozoic to Low Paleozoic Erathem, Sichuan Basin, Chengdu University of Technology 174 p.

Tang, J., T. Zhang, Z. Bao, and M. Zhang, 2004, Study of Organic Inclusion in the Carbonate Reservoir Bed of the Weiyuan Gas Field in the Sichuan Basin: Geological Review, v. 50, p. 210-214.

Teinturier, S., J. Pironon, and F. Walgenwitz, 2002, Fluid inclusions and PVTX modelling: examples from the Garn Formation in well 6507/2-2, Haltenbanken, Mid-Norway: Marine and Petroleum Geology, v. 19, p. 755-765, doi: 10.1016/S0264-8172(02)00055-7.

Tian, Y., B. P. Kohn, C. Zhu, M. Xu, S. Hu, and A. J. W. Gleadow, 2012, Post-orogenic evolution of the Mesozoic Micang Shan Foreland Basin system, central China: Basin Research, v. 24, p. 70–90, doi: 10.1111/j.1365-2117.2011.00516.x.

Tissot, B., 1984, Recent advances in petroleum geochemistry applied to hydrocarbon exploration: AAPG Bulletin, v. 68, p. 545-563, doi: 10.1306/AD461336-16F7-11D7-8645000102C1865D.

Tissot, B., R. Pelet, and P. Ungerer, 1987, Thermal history of sedimentary basins, maturation indices, and kinetics of oil and gas generation: AAPG Bulletin, v. 71, p. 1445-1466.

Tissot, B. P., and D. H. Welte, 1984, Diagenesis, Catagenesis and Metagenesis of Organic Matter, Petroleum Formation and Occurrence: Berlin, Heidelberg, Springer Berlin Heidelberg, p. 69-73.

Tohver, E., A. Weil, J. Solum, and C. Hall, 2008, Direct dating of carbonate remagnetization by 40 Ar/39 Ar analysis of the smectite–illite transformation: Earth and Planetary Science Letters, v. 274, p. 524-530, doi: 10.1016/j.epsl.2008.08.002.

Tsuzuki, N., N. Takeda, M. Suzuki, and K. Yokoi, 1999, The kinetic modeling of oil cracking by hydrothermal pyrolysis experiments: International Journal of Coal Geology, v. 39, p. 227-250, doi: 10.1016/S0166-5162(98)00047-0.

Vandenbroucke, M., F. Behar, and J. Rudkiewicz, 1999, Kinetic modelling of petroleum formation and cracking: implications from the high pressure/high temperature Elgin Field (UK, North Sea): Organic Geochemistry, v. 30, p. 1105-1125, doi: 10.1016/S0146-6380(99)00089-3.

Wang, D., and G. Wang, 2011, Fromation and Evolution of High-quality Dolomite Reservoir in Dengying Formation of Sichuan, NanJiang Area, Sichuan: Geoscience, v. 25, p. 660-667.

Wang, G., N. Li, B. Gao, X. Li, S. Shi, and T. Wang, 2013, Thermochemical sulfate reduction in fossil Ordovician deposits of the Majiang area: Evidence from a molecular-marker investigation: Chinese Science Bulletin, v. 58, p. 3588-3594, doi: 10.1007/s11434-013-5843-x.

Wang, G., S. Liu, N. Li, D. Wang, and Y. Gao, 2014, Formation and preservation mechanism of high quality reservoir in deep burial dolomite in the Dengying Formation on the northern margin of the Sichuan basin: Acta Petrolei Sinica, v. 30, p. 667-678.

Wang, J., 2015, Fluid Flow Analysis of Sinian Reservoir in the Micangshan Tectonic Belt, China University of Geoscience (Wuhan), 26 p.

Wang, X., C. Xue, Z. Li, Q. Li, and R. Yang, 2008, Geological and geochemical characteristics of Mayuan Pb-Zn ore deposit on northern margin of Yangtze landmass: Mineral Deposits, v. 27, p. 37-48.

Waples, D. W., 2000, The kinetics of in-reservoir oil destruction and gas formation: constraints from experimental and empirical data, and from thermodynamics: Organic Geochemistry, v. 31, p. 553-575, doi: 10.1016/S0146-6380(00)00023-1.

Wei, G., G. Chen, S. Du, L. Zhang, and W. Yang, 2008, Petroleum systems of the oldest gas field in China: Neoproterozoic gas pools in the Weiyuan gas field, Sichuan Basin: Marine and Petroleum Geology, v. 25, p. 371-386, doi: 10.1016/j.marpetgeo.2008.01.009.

Wu, Z., P. Peng, J. Fu, G. Sheng, and D. Liu, 2000, Bitumen associated with petroleum formation, evolution and alteration-review and case studies in China: Developments in petroleum science, p. 401-443, doi: 10.1016/S0376-7361(09)70286-9.

Xiao, X. M., F. Wang, R. W. T. Wilkins, and Z. G. Song, 2007, Origin and gas potential of pyrobitumen in the Upper Proterozoic strata from the Middle Paleo-Uplift of the Sichuan Basin, China: International Journal of Coal Geology, v. 70, p. 264-276, doi: 10.1016/j.coal.2006.03.007.

Xu, G., J. L. Hannah, H. J. Stein, B. Bingen, G. Yang, A. Zimmerman, W. Weitschat,

A. Mørk, and H. M. Weiss, 2009a, Re–Os geochronology of Arctic black shales to evaluate the Anisian–Ladinian boundary and global faunal correlations: Earth and Planetary Science Letters, v. 288, p. 581-587, doi: 10.1016/j.epsl.2009.10.022.

Xu, G., J. L. Hannah, H. J. Stein, A. Mørk, J. O. Vigran, B. Bingen, D. L. Schutt, and B. A. Lundschien, 2014, Cause of Upper Triassic climate crisis revealed by Re–Os geochemistry of Boreal black shales: Palaeogeography, Palaeoclimatology, Palaeoecology, v. 395, p. 222-232, doi: 10.1016/j.palaeo.2013.12.027.

Xu, H., S. Liu, G. Qu, Y. Li, G. Sun, and K. Liu, 2009b, Structural Characteristics and Formation Mechanism in the Micangshan Foreland,South China: Acta Geologica Sinica, v. 83, p. 81-91.

Yang, P., Z. Wang, F. Yin, J. Liu, J. Lin, D. Zhang, and X. Huang, 2014, Identification of oil resource and analysis of hydrocarbon migration and accumulation of Majiang Paleo-reservoir: Evidence from oil-gas Geochemistry: Geology in China, v. 41, p. 982-994.

Yang, Z., L. Ratschbacher, R. Jonckheere, E. Enkelmann, Y. Dong, C. Shen, M. Wiesinger, and Q. Zhang, 2013, Late-stage foreland growth of China's largest orogens (Qinling, Tibet): Evidence from the Hannan-Micang crystalline massifs and the northern Sichuan Basin, central China: Lithosphere, v. 5, p. 420-437, doi: 10.1130/L260.1

Yin, A., and S. Nie, 1993, An indentation model for the North and South China collision and the development of the Tan‐Lu and Honam Fault Systems, eastern Asia: Tectonics, v. 12, p. 801-813, doi: 10.1029/93TC00313.

Yuan, H., J. Liang, D. Gong, G. Xu, S. Liu, and G. Wang, 2012, Formation and evolution of Sinian oil and gas pools in typical structures, Sichuan Basin, China: Petroleum Science, v. 9, p. 129-140, doi: 10.1007/s12182-012-0193-x.

Zhang, S., 2013, The characteristics of natural bitumen and analysis of source rock of lead-zinc deposit of Deying Formation in north Sichuan basin, Chang'an University, 76 p.

Zhang, S., and G. Zhu, 2006, Gas accumulation characteristics and exploration potential of marine sediments in Sichuan Basin: Acta Petrolei Sinica, v. 27, p. 1-8.

Zhang, X., and G. Li, 1999, The relationship between distributuion of natural asphal oil and gas seepage and exploration in South China: Journal of Southwest Petroleum Institute, v. 21, p. 36-40.

Zhang, Z., 1988, Pyrobitumen feature and method on measuring its reflectance: Xinjiang Petroleum Geology, v. 9, p. 24-29.

Zhao, Z., Y. Zhu, and Y. Xu, 2004, Fromation and Predication of Exploration Targets of Paleozoic-Mesozoic Oil-Gas Reservoirs in South China: Acta Geology Sinica, v. 78, p. 710-720.

Zhu, G., S. Zhang, Y. Liang, Y. Ma, J. Dai, J. Li, and G. Zhou, 2006, The characteristics of natural gas in Sichuan basin and its sources: Earth Science Frontiers, v. 13, p. 234-248.

Zou, C., J. Du, C. Xu, Z. Wang, B. Zhang, G. Wei, T. Wang, G. Yao, S. Deng, and J. Liu, 2014a, Formation, distribution, resource potential, and discovery of Sinian–Cambrian giant gas field, Sichuan Basin, SW China: Petroleum Exploration and Development, v. 41, p. 306-325.

Zou, C., G. Wei, C. Xu, J. Du, Z. Xie, Z. Wang, L. Hou, C. Yang, J. Li, and W. Yang, 2014b, Geochemistry of the Sinian–Cambrian gas system in the Sichuan Basin, China: Organic Geochemistry, v. 74, p. 13-21, doi: 10.1016/j.orggeochem.2014.03.004.

Author's vita

Xiang Ge

Key Laboratory of Tectonics and Petroleum Resources (China University of Geosciences), Ministry of Education, Wuhan, 430074, China; 388 Lumo Road, Hongshan District, Wuhan City, Hubei Province, China.

xiangge89@126.com

Xiang Ge is a Joint Ph.D student at the China University of Geoscience (Wuhan) and Durham University. He received his B.Sc. and M.Sc. from China University of Geoscience (Wuhan). His PhD thesis is focusing on the petroleum geology of the Sichuan Basin applying hydrocarbon Re-Os isotope, structural and tectonic analyses.

Chuanbo Shen (*Corresponding author)

Key Laboratory of Tectonics and Petroleum Resources (China University of Geosciences), Ministry of Education, Wuhan, 430074, China; 388 Lumo Road, Hongshan District, Wuhan City, Hubei Province, China.

cugshen@126.com

Chuanbo Shen (Corresponding author) is currently a professor in the Faculty of Earth Resources at the China University of Geosciences (Wuhan). He received his B.Sc., M.Sc., and Ph.D. from China University of Geoscience (Wuhan). He also completed postdoctoral research in Technische Universität Bergakademie Freiberg, Germany. His present research interests are low-temperature thermochronology, tectonic-thermal evolution and hydrocarbon geochronology.

David Selby

Department of Earth Sciences, Durham University, Durham, DH1 3LE, UK

david.selby@durham.ac.uk

David Selby is a Professor of Earth Sciences at Durham University, UK. He received a bachelor’s degree in geology from Southampton University, UK and Ph.D. degree from the University of Alberta, Canada. He also carried out his postdoctoral research at the University of Alberta. His research focuses on the Earth Science disciplines of economic geology, petroleum geoscience and paleoclimate / oceanography, principally through the application and development of the novel, state-of-the-art, rhenium-osmium radio isotope methodology.

Guozhi Wang

Faculty of Earth Sciences, Chengdu University of Technology, Chengdu, 610059, China; No.1 Erxianqiao road, Chenghua District, Chengdu City, Sichuan Province, China.

wangguozhi66@163.com

Guozhi Wang is a Professor of the Earth Science Faculty of the Chengdu University of Technology. He obtained his bachelor degree from Chuangchun Geological College in 1986, and M.Sc degree and Ph.D from Chengdu University of Technology in 1989 and 2000, respectively. His present research interests include basin analysis, isotopic dating, structure analysis of orogenic belts and sedimentary basins.

Zhao Yang

Department of Geology, Northwest University, Xi’an, 710069, China, No.229 North Taibai Road, Xi’an City, Shanxi Province, China

jdmuyi@sina.com

Zhao Yang is currently a lecture in the Department of Geology at the Northwest University, China. He received his bachelor and master degree from Northwest University, China, and Ph.D degree from Technische Universität Bergakademie Freiberg, Germany. His present research focus on using low temperature thermochronology to quantify the post orogenic process and landscape evolution.

Yongjun Gong

Key Laboratory of Tectonics and Petroleum Resources (China University of Geosciences), Ministry of Education, Wuhan, 430074, China; 388 Lumo Road, Hongshan District, Wuhan City, Hubei Province, China.

gyjxhz@163.com

Yongjun Gong is currently a lecturer in the Faculty of Earth Resources at the China University of Geosciences (Wuhan). He received his B.Sc., M.Sc. and Ph.D degree from China University of Geoscience (Wuhan). His present research interests include economic geology, structural geology.

Suofei Xiong

State Key Laboratory of Geological Processes and Mineral Resources, Faculty of Earth Resources and Collaborative Innovation Center for Exploration of Strategic Mineral Resources, China University of Geosciences, Wuhan 430074, China; 388 Lumo Road, Hongshan District, Wuhan, Hubei Province, China.

Sophie_0913@foxmail.com

Suofei Xiong is currently a postdoctoral research in the Collaborative Innovation Center for Exploration of Strategic Mineral Resources, China University of Geosciences (Wuhan), and her postdoctoral research work focuses on the isotopic geochemistry of Pb-Zn deposits. She received her B.Sc., M.Sc., and Ph.D. from China University of Geoscience (Wuhan).

Figure Captions

Fig. 1. Simplified map of the Sichuan Basin showing the distribution of oil and gas fields (Substantially modified from Li et al., 2015; Li et al., 2001; Ma et al., 2010).

Fig. 2. Simplified geological map of the Micang Shan Uplift, northern Sichuan Basin. (A) Regional map of the Micang Shan Uplift and its adjacent area, Longmen Shan Orogeny, Hannan Uplift and Daba Orogen in the west, northeast, east, respectively. (B)

Simplified geologic and structural map of Micang Shan Uplift, northern Sichuan Basin (Substantially modified from Wang et al., 2014), showing the location of both bitumen and the AFT samples.

Fig. 3. Combined stratigraphic sequences, petroleum system and tectonic events in the northern Sichuan Basin (Substantially modified from Huang, 2013; Huang, 2010; Wang, 2015).

Fig. 4. Examples of pyrobitumen outcropping in the Jiulingzi (JLZ), Nanmushu (NMS), Kongxigou (KXG) and Yangba (YB) areas.

Fig. 5. Petrography of the pyrobitumen of this study: (A) and (B) from the Nanmushu 1070 area; (C) and (D) from the Nanmushu 1030 area; and (E) and (F) from the Jiulingzi area.

Fig.6. A. Re-Os isochron plot showing all the data in the Micang Shan Uplift; B. Plot of percent deviation from the 239 Ma best-fit line; C. Re-Os isotope data of bitumen from Mayuan, Nanmushu and Zhujiaba area with Osi$_{239}$ from 2.25 - 2.30. Data-point ellipses shown with 2-sigma (2σ) absolute uncertainty (sigma (σ) is the standard deviation of the age). MSWD is short for Mean Square Weight Deviation. Data labels are sample numbers listed in Table 1.

Fig. 7. Collected apatite fission track (AFT) thermal history modeling results from the Micang Shan Uplift and inner Sichuan Basin (Substantially modified from Tian et al., 2012; Yang et al., 2013). D: determinted apatite fission track age; M: modeled apatite fission track age; GOF: goodness of fit; N: number of measured fission track; Lm: mean length of the measured fission track length; SD: standard deviation.

Fig. 8. A. Basin modelling and fluid inclusion results for the Micang Shan Uplift, showing the key time for gas generation. B. Cartoon model showing the hydrocarbon evolution of the Micang Shan Uplift, north Sichuan Basin: (a) original hydrocarbon reservoir formation process prior to the Silurian; (b) pyrobitumen and dry gas formation by thermal cracking during the Jurassic; and (c) reservoir alteration and erosion during the Cretaceous Yanshan orogeny.

Table 1. Re-Os isotopic and BRo data of the solid bitumen from the Micang Shan Uplift, North Sichuan Basin

Table 2. Apatite fission track data from the Micang Shan Uplift and inner Sichuan Basin

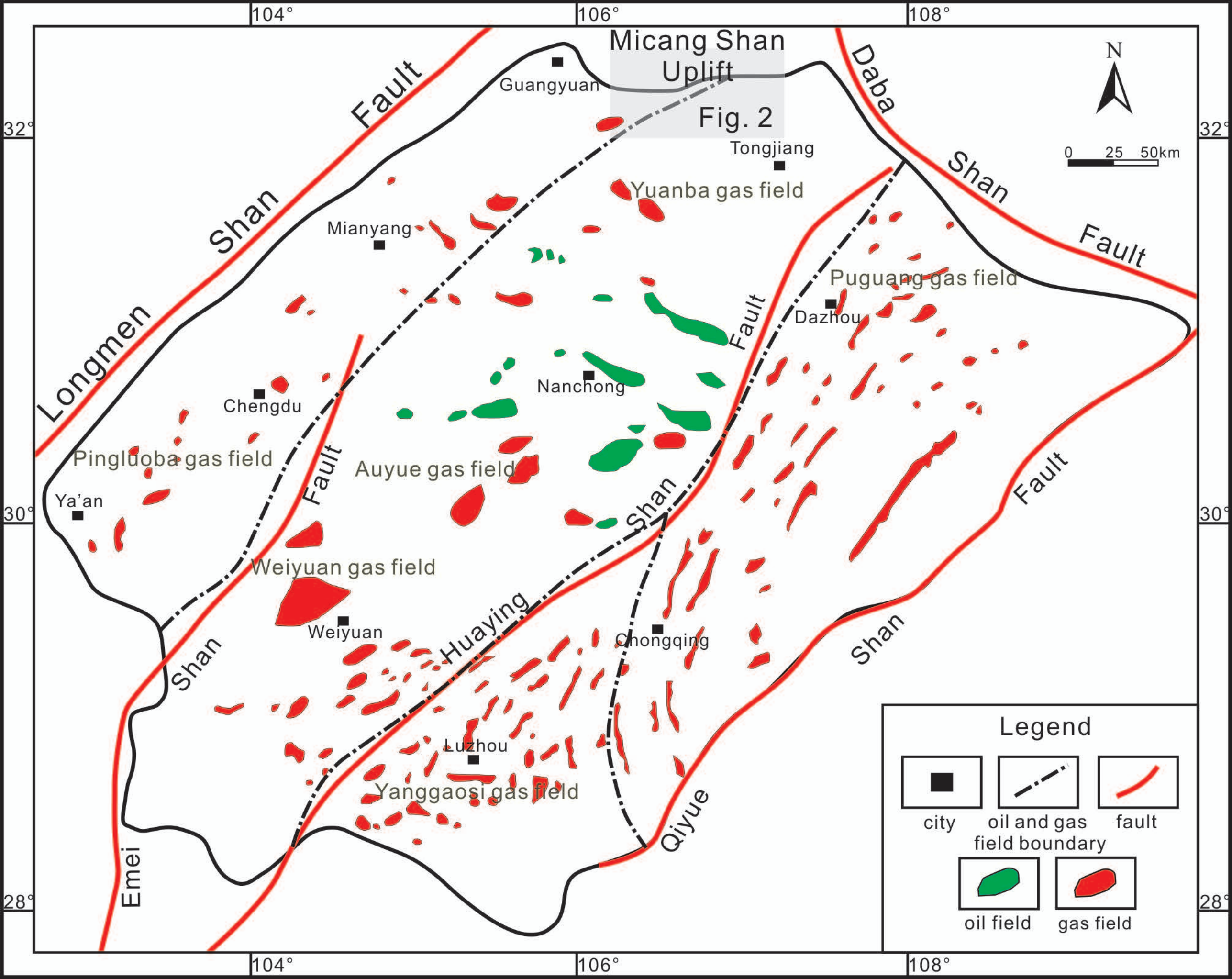
104°
106°
108°
32°
30°
28°
Micang Shan Uplift
Fig. 2
N
0 25 50km
Longmen Shan Fault
Daba Shan Fault
Guangyuan
Tongjiang
Yuanba gas field
Mianyang
Puguang gas field
Dazhou
Fault
Nanchong
Chengdu
Pingluoba gas field
Auyue gas field
Fault
Ya'an
Huaying Shan
Weiyuan gas field
Weiyuan
Chongqing
Shan
Fault
Shan
Luzhou
Yanggaosi gas field
Emei Shan
Qiyue
Legend
city
oil and gas field boundary
fault
oil field
gas field

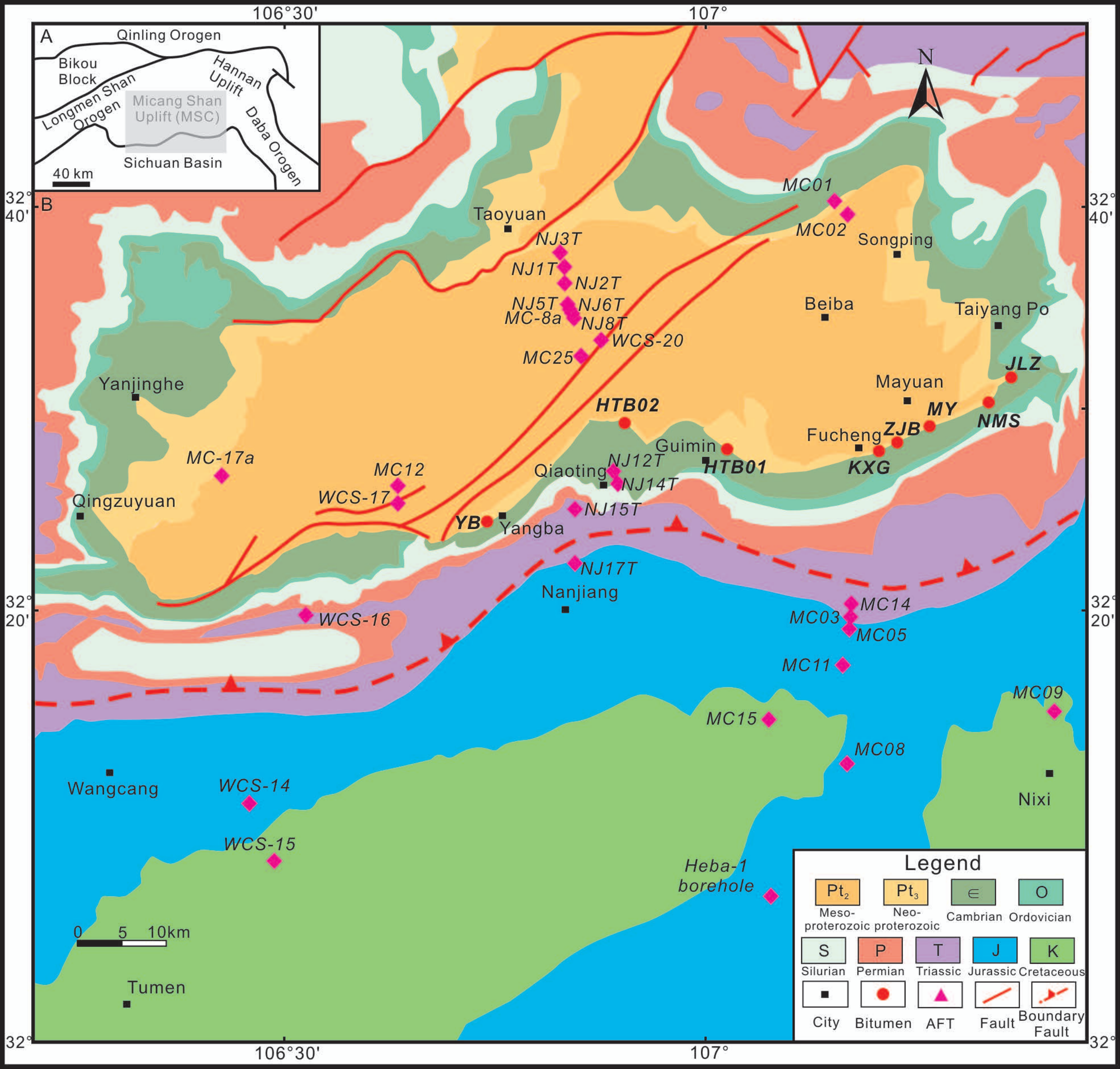

106°30'
107°
A
Qinling Orogen
Bikou Block
Hannan Uplift
Longmen Shan Orogen
Micang Shan Uplift (MSC)
Daba Orogen
Sichuan Basin
40 km
B
32° 40'
32° 20'
32°
N
Taoyuan
Songping
Beiba
Taiyang Po
Mayuan
Fucheng
Guimin
Qiaoting
Yangba
Nanjiang
Yanjinghe
Qingzuyuan
Wangcang
Tumen
Nixi
MC01
MC02
NJ3T
NJ1T
NJ2T
NJ5T
NJ6T
MC-8a
NJ8T
WCS-20
MC25
JLZ
MY
NMS
ZJB
KXG
HTB02
HTB01
MC-17a
MC12
WCS-17
NJ12T
NJ14T
NJ15T
YB
NJ17T
WCS-16
MC14
MC03
MC05
MC11
MC09
MC15
MC08
WCS-14
WCS-15
Heba-1 borehole
0 5 10km
Legend
Pt_2 Meso-proterozoic
Pt_3 Neo-proterozoic
∈ Cambrian
O Ordovician
S Silurian
P Permian
T Triassic
J Jurassic
K Cretaceous
City
Bitumen
AFT
Fault
Boundary Fault

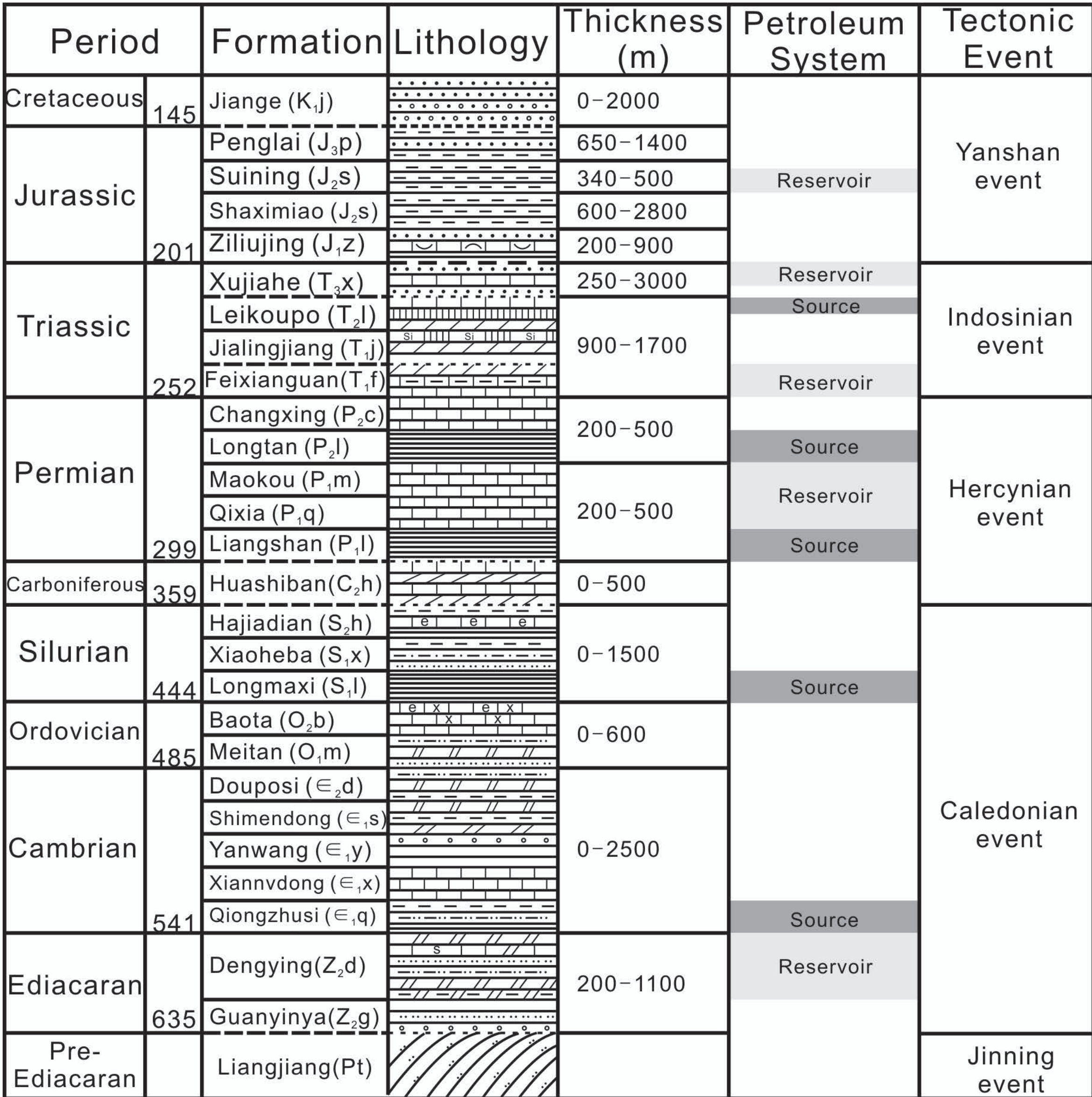

Period
Formation
Lithology
Thickness (m)
Petroleum System
Tectonic Event
Cretaceous
145
Jiange (K_1j)
0–2000
Jurassic
201
Penglai (J_3p)
650–1400
Suining (J_2s)
340–500
Reservoir
Shaximiao (J_2s)
600–2800
Ziliujing (J_1z)
200–900
Yanshan event
Triassic
252
Xujiahe (T_3x)
250–3000
Reservoir
Leikoupo (T_2l)
Source
Jialingjiang (T_1j)
900–1700
Si
Feixianguan(T_1f)
Reservoir
Indosinian event
Permian
299
Changxing (P_2c)
200–500
Longtan (P_2l)
Source
Maokou (P_1m)
Reservoir
Qixia (P_1q)
200–500
Liangshan (P_1l)
Source
Hercynian event
Carboniferous
359
Huashiban(C_2h)
0–500
Silurian
444
Hajiadian (S_2h)
e
Xiaoheba (S_1x)
0–1500
Longmaxi (S_1l)
Source
Ordovician
485
Baota (O_2b)
e x
Meitan (O_1m)
0–600
Cambrian
541
Douposi ($\in_2d$)
Shimendong ($\in_1s$)
Yanwang ($\in_1y$)
0–2500
Xiannvdong ($\in_1x$)
Qiongzhusi ($\in_1q$)
Source
Caledonian event
Ediacaran
635
Dengying(Z_2d)
s
Reservoir
200–1100
Guanyinya(Z_2g)
Pre-Ediacaran
Liangjiang(Pt)
Jinning event

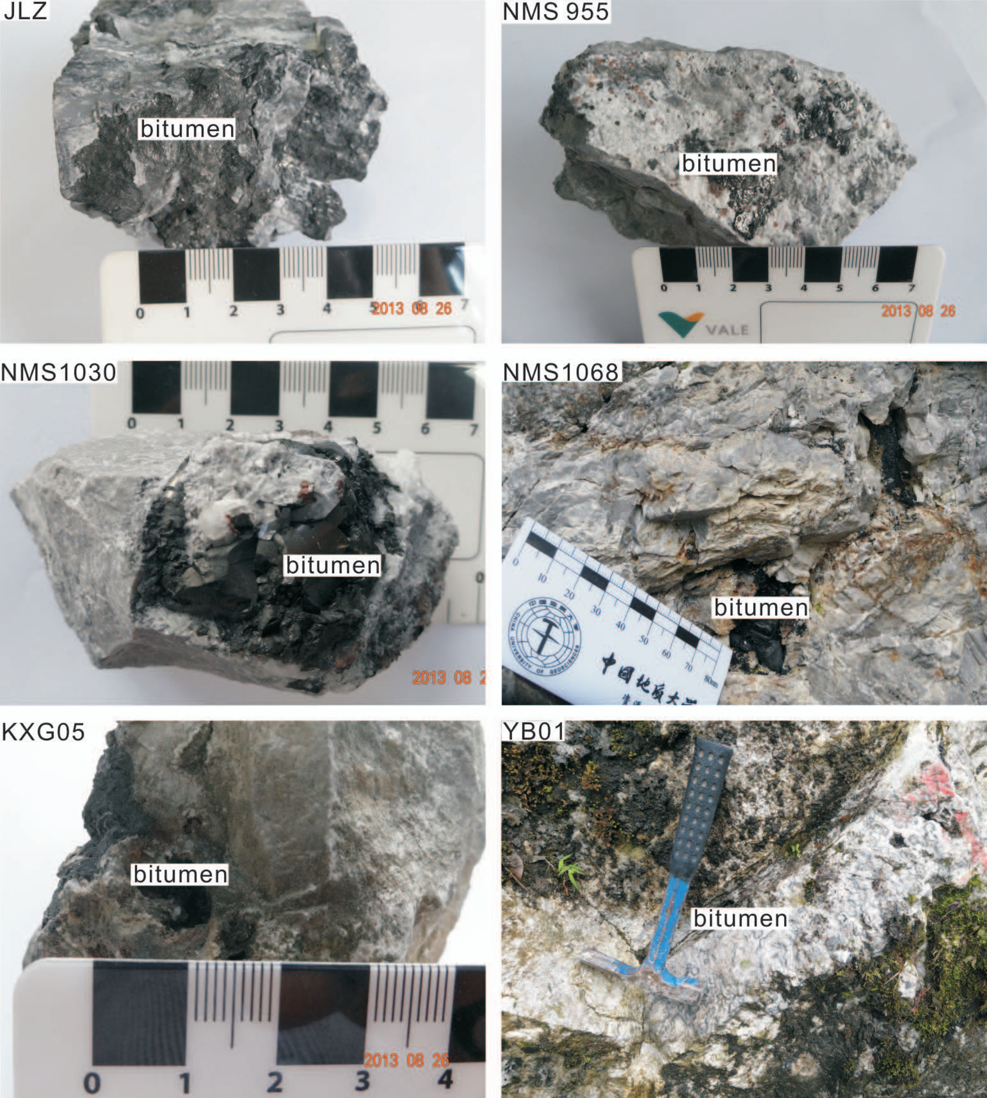
JLZ
bitumen
2013 08 26
NMS 955
bitumen
VALE
2013 08 26
NMS1030
bitumen
NMS1068
bitumen
中国地质大学
KXG05
bitumen
2013 08 26
YB01
bitumen

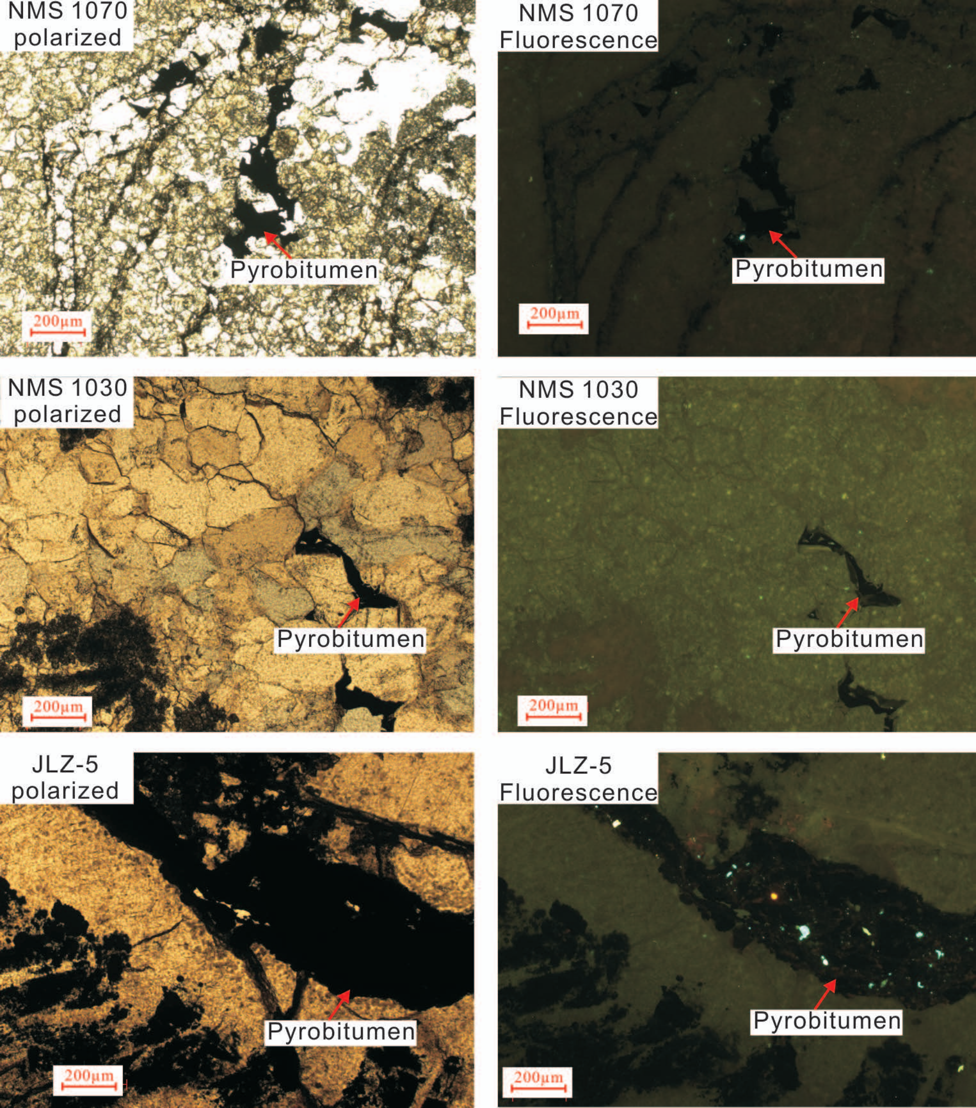
NMS 1070
polarized
Pyrobitumen
200μm
NMS 1070
Fluorescence
Pyrobitumen
200μm
NMS 1030
polarized
Pyrobitumen
200μm
NMS 1030
Fluorescence
Pyrobitumen
200μm
JLZ-5
polarized
Pyrobitumen
200μm
JLZ-5
Fluorescence
Pyrobitumen
200μm

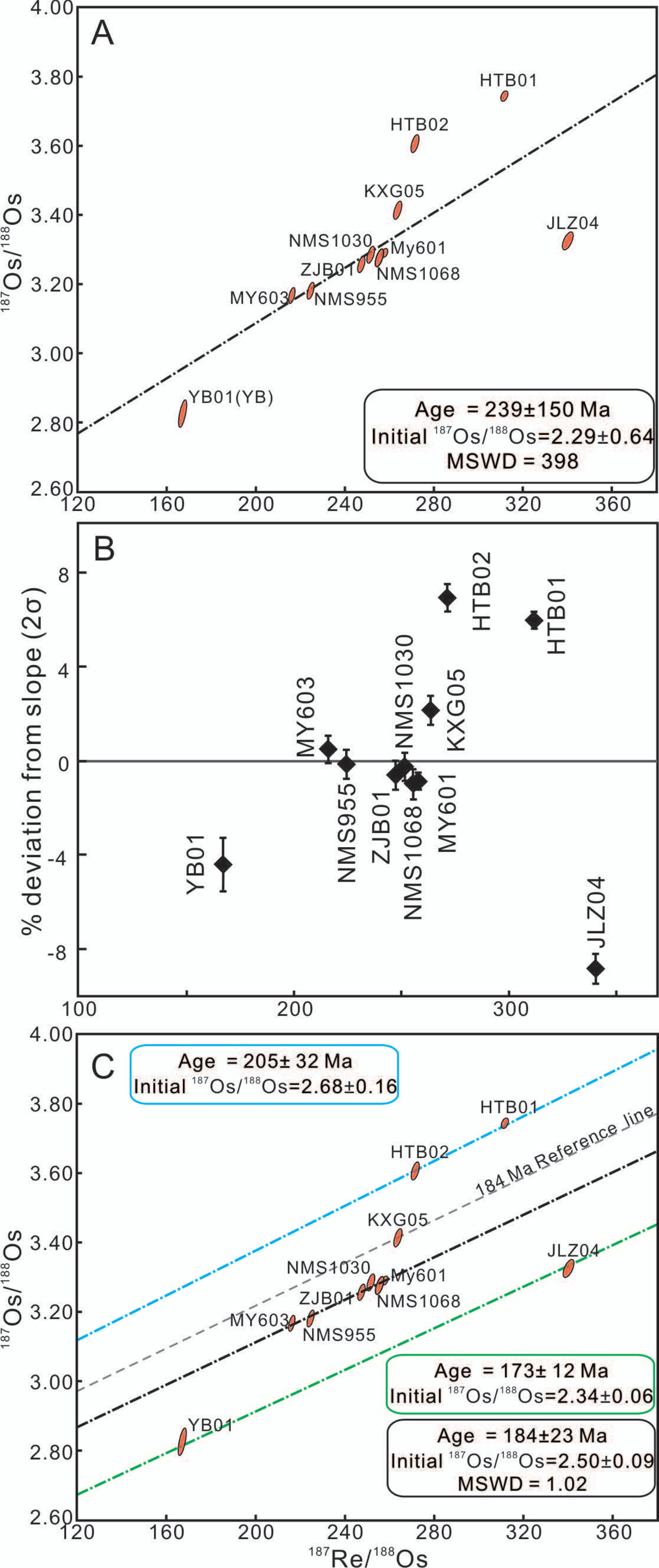

A
HTB01
HTB02
KXG05
JLZ04
NMS1030
My601
ZJB01
NMS1068
MY603
NMS955
YB01(YB)
Age = 239±150 Ma
Initial $^{187}Os/^{188}Os$=2.29±0.64
MSWD = 398
$^{187}Os/^{188}Os$
B
% deviation from slope (2σ)
HTB02
HTB01
MY603
NMS1030
KXG05
NMS955
ZJB01
NMS1068
MY601
YB01
JLZ04
C
Age = 205± 32 Ma
Initial $^{187}Os/^{188}Os$=2.68±0.16
184 Ma Reference line
Age = 173± 12 Ma
Initial $^{187}Os/^{188}Os$=2.34±0.06
Age = 184±23 Ma
Initial $^{187}Os/^{188}Os$=2.50±0.09
MSWD = 1.02
$^{187}Re/^{188}Os$

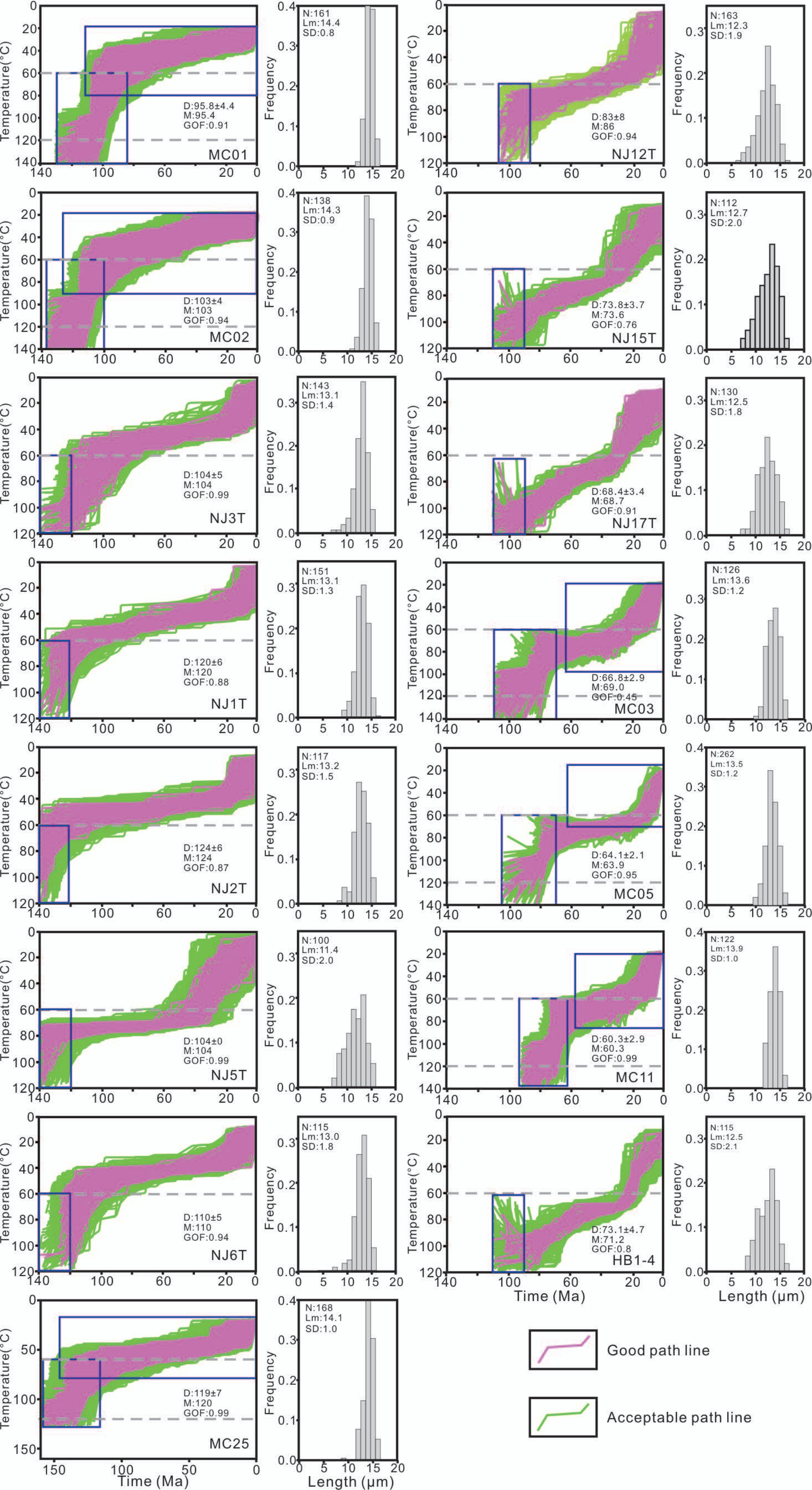

MC01
D:95.8±4.4
M:95.4
GOF:0.91
N:161
Lm:14.4
SD:0.8
NJ12T
D:83±8
M:86
GOF:0.94
N:163
Lm:12.3
SD:1.9
MC02
D:103±4
M:103
GOF:0.94
N:138
Lm:14.3
SD:0.9
NJ15T
D:73.8±3.7
M:73.6
GOF:0.76
N:112
Lm:12.7
SD:2.0
NJ3T
D:104±5
M:104
GOF:0.99
N:143
Lm:13.1
SD:1.4
NJ17T
D:68.4±3.4
M:68.7
GOF:0.91
N:130
Lm:12.5
SD:1.8
NJ1T
D:120±6
M:120
GOF:0.88
N:151
Lm:13.1
SD:1.3
MC03
D:66.8±2.9
M:69.0
GOF:0.45
N:126
Lm:13.6
SD:1.2
NJ2T
D:124±6
M:124
GOF:0.87
N:117
Lm:13.2
SD:1.5
MC05
D:64.1±2.1
M:63.9
GOF:0.95
N:262
Lm:13.5
SD:1.2
NJ5T
D:104±0
M:104
GOF:0.99
N:100
Lm:11.4
SD:2.0
MC11
D:60.3±2.9
M:60.3
GOF:0.99
N:122
Lm:13.9
SD:1.0
NJ6T
D:110±5
M:110
GOF:0.94
N:115
Lm:13.0
SD:1.8
HB1-4
D:73.1±4.7
M:71.2
GOF:0.8
N:115
Lm:12.5
SD:2.1
MC25
D:119±7
M:120
GOF:0.99
N:168
Lm:14.1
SD:1.0
Temperature(°C)
Frequency
Time (Ma)
Length (μm)
Good path line
Acceptable path line

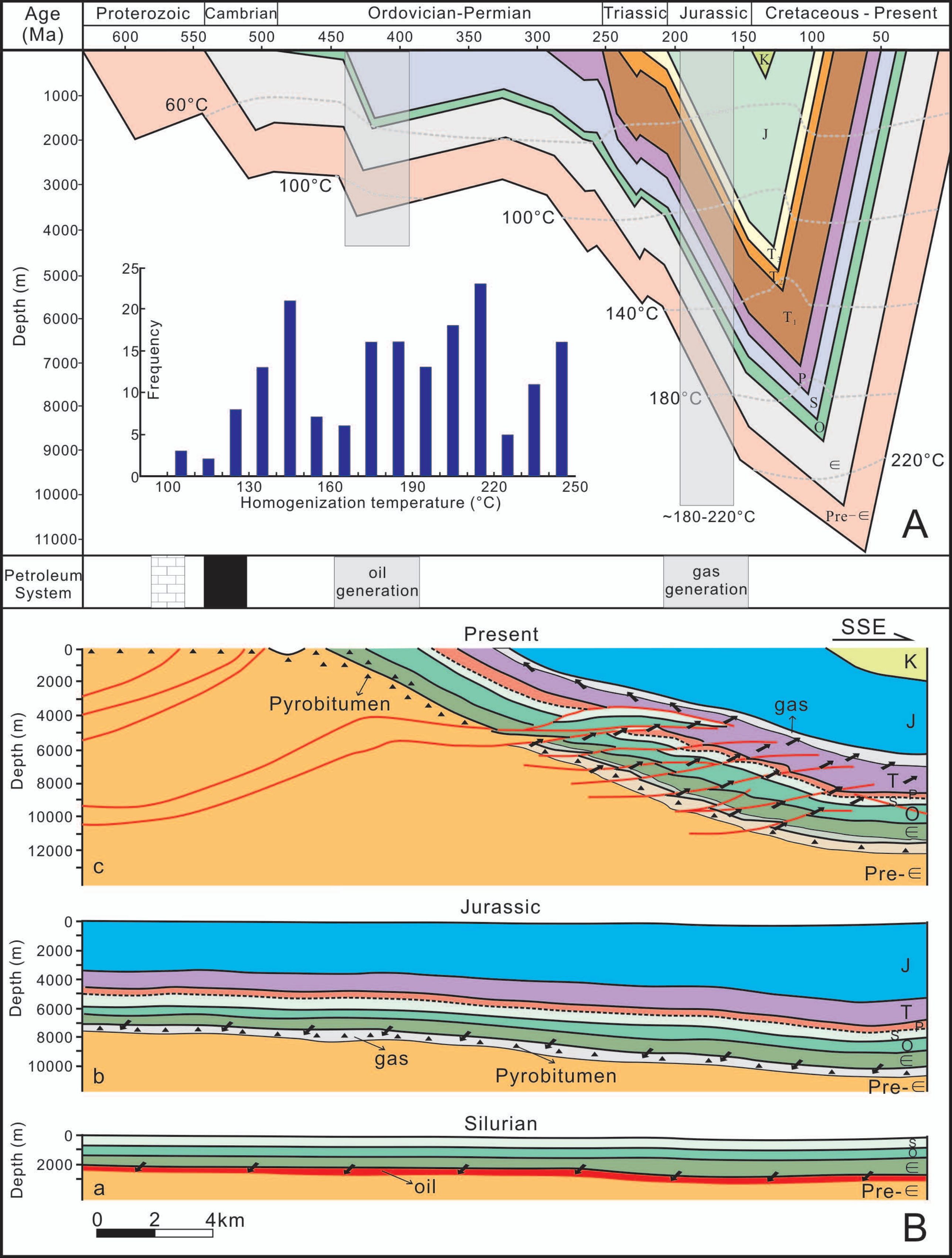

Age (Ma)
Proterozoic
Cambrian
Ordovician-Permian
Triassic
Jurassic
Cretaceous - Present
600 550 500 450 400 350 300 250 200 150 100 50
Depth (m)
60°C
100°C
100°C
140°C
180°C
220°C
~180-220°C
K
J
T3
T2
T1
P
S
O
∈
Pre-∈
Frequency
Homogenization temperature (°C)
A
Petroleum System
oil generation
gas generation
Present
SSE
Pyrobitumen
gas
T
c
Jurassic
gas
Pyrobitumen
b
Silurian
oil
a
0 2 4km
B

Table 1.Re-Os isotopic data on the bitumen from the Micang Shan Uplift, North Sichuan Basin

Sample name	Latitude	Longitude	Strata	BRo (%)	Re (ppb)	±	Os (ppt)	±	$^{187}Re/^{188}Os$	±	$^{187}Os/^{188}Os$	±	rho	Osi (239Ma)
HTB01	32°28'58"	107°05'39"	Dengying formation	/	179.5	0.6	4087.2	18.6	311.6	1.3	3.746	0.012	0.419	2.502
HTB02	32°30'02"	106°52'42"	Dengying formation	/	177.4	0.6	4579.2	28.3	271.4	1.5	3.608	0.021	0.554	2.525
MY601	32°31'32"	107°19'08"	Dengying formation	/	191.4	0.7	5053.0	21.7	257.8	1.0	3.291	0.010	0.391	2.263
MY603	32°31'28"	107°18'54"	Dengying formation	/	154.8	0.5	4823.7	28.7	216.0	1.2	3.168	0.019	0.552	2.306
NMS955	32°31'28"	107°18'56"	Dengying formation	3.97	143.5	0.5	4307.0	26.5	224.4	1.3	3.182	0.020	0.591	2.286
NMS1030	32°31'48"	107°19'38"	Dengying formation	3.94	184.9	0.6	5002.3	30.6	251.5	1.4	3.286	0.020	0.580	2.283
NMS1068	32°31'41"	107°19'42"	Dengying formation	3.25	113.8	0.4	3030.4	19.1	255.4	1.5	3.277	0.021	0.625	2.258
ZJB01	32°29'52"	107°09'54"	Dengying formation	/	153.8	0.5	4220.9	25.3	247.2	1.3	3.258	0.019	0.555	2.271
JLZ04	32°32'11"	107°19'48"	Dengying formation	4.08	188.1	0.7	3777.1	23.8	340.2	2.0	3.326	0.021	0.606	1.969
YB01	32°28'19"	106°47'10"	Dengying formation	/	145.2	0.5	5669.5	47.4	166.8	1.5	2.826	0.032	0.653	2.160
KXG05	32°29'39"	107°09'35"	Dengying formation	3.97	106.2	0.6	4812.9	30.4	263.6	1.5	3.415	0.021	0.585	2.363

Footnotes: BRo = Bitumen reflectance; Re (ppb) = rhenium (part per billion); Os (ppt) = Osmium (parts per trillion); $^{187}Re/^{188}Os$ = ^{187}rhenium/^{188}Osmium; $^{187}Os/^{188}Os$ = ^{187}Osmium /^{188}Osmium; rho = the associated error correlation of the $^{187}Re/^{188}Os$ and $^{187}Os/^{188}Os$; Osi(239Ma) = initial $^{187}Os/^{188}Os$ ratio at 239 Ma.

Table. 2 Apatite fission track data from the Micang Shan Uplift inner Sichuan Basin

AFT sample	Latitude	Longitude	Lithology	Strata	Elevation (m)(ft)	AFT age (Ma)	±	Length (μm)	±	Ref
Uplift										
MC01	32°41'54"	107°07'27"	Granite	Proterozoic	1106(3628)	95.8	4.4	13.00	0.10	Yang et al., 2013
MC02	32°41'17"	107°08'24"	Granite	Proterozoic	1073(3520	103.0	3.7	12.90	0.10	Yang et al., 2013
NJ3T	32°37'12"	106°49'30"	Diorite	Proterozoic	1650(5413)	103.0	5.1	13.14	0.12	Tian et al., 2011
NJ1T	32°36'58"	106°49'41"	Diorite	Proterozoic	1554(5098)	119.8	5.9	13.13	0.10	Tian et al., 2011
NJ2T	32°36'36"	106°49'48"	Diorite	Proterozoic	1588(5210)	123.5	6	13.23	0.10	Tian et al., 2011
NJ5T	32°35'42"	106°50'28"	Diorite	Proterozoic	1268(4160)	103.7	4.2	11.40	0.25	Tian et al., 2011
NJ6T	32°35'28"	106°50'28"	Sandstone	Proterozoic	1286(4219)	110.1	5.3	12.95	0.12	Tian et al., 2011
MC-8a	32°35'22"	106°50'40"	Diorite	Proterozoic	1269(4163)	99.0	/	/		Sun, 2011
NJ8T	32°34'26"	106°50'42"	Siltstone	Pre-cambrian	1259(4130)	93.9	4.1	/	/	Tian et al., 2011
WCS-20	32°33'09"	106°52'11"	Granite	Proterozoic	703(2306)	63.7	6.4	12.10	0.20	Lei et al., 2012
MC25	32°32'45"	106°51'53"	Granite	Proterozoic	1317(4321)	110.7	6.8	12.80	0.10	Yang et al., 2013
Basin										
NJ12T	32°28'26"	106°52'44"	Sandstone	Ordovician	636(2087)	82.9	7.8	12.25	0.17	Tian et al., 2011
MC-17a	32°28'19"	106°26'44"	Diorite	Proterozoic	625(2050)	81.0	/	/	/	Sun, 2011
NJ14T	32°27'18"	106°53'20"	Sandstone	Silurian	575(1886)	60.8	5.7	/	/	Tian et al., 2011
MC12	32°26'50"	106°38'37"	Diorite	Proterozoic	978(3209)	68.9	3.5	/	/	Yang et al., 2013
WCS-17	32°26'02"	106°38'38"	Conglomerate	Cambrian	1139(3736)	80.4	10.6	12.10	0.20	Lei et al., 2012
NJ15T	32°25'30"	106°51'50"	Sandstone	Triassic	506(1660)	73.8	3.7	12.66	0.20	Tian et al., 2011
NJ17T	32°22'19"	106°51'11"	Sandstone	Jurassic	557(1827)	68.4	3.4	12.49	0.16	Tian et al., 2011
MC14	32°21'39"	107°10'17"	Sandstone	Jurassic	500(1640)	62.4	5.2	/	/	Yang et al., 2013
MC03	32°21'07"	107°10'06"	Sandstone	Triassic	515(1690)	66.8	2.9	11.80	0.20	Yang et al., 2013
MC04	32°20'51"	107°10'37"	Sandstone	Jurassic	550(1804)	78.2	5.8	/	/	Yang et al., 2013
MC05	32°19'31"	107°10'44"	Sandstone	Jurassic	505(1657)	64.1	2.1	11.50	0.10	Yang et al., 2013
WCS-16	32°19'17"	106°32'13"	Conglomerate	Cambrian	541(1775)	69.8	6.2	11.40	0.30	Lei et al., 2012
MC11	32°17'56"	107°09'32"	Sandstone	Triassic	497(1631)	61.6	3	12.20	0.20	Yang et al., 2013
MC09	32°15'26"	107°26'05"	Sandstone	Cretaceous	448(1470)	60.3	2.3	/	/	Yang et al., 2013
MC15	32°14'52"	106°58'30"	Sandstone	Cretaceous	461(1512)	66.8	2.5	12.20	0.20	Yang et al., 2013
MC08	32°13'06"	107°10'41"	Sandstone	Jurassic	481(1578)	70.2	4.5	/	/	Yang et al., 2013
WCS-14	32°11'34"	106°27'50"	sandstone	Jurassic	462(1516)	70.7	4.7	10.60	0.30	Lei et al., 2012
WCS-15	32°08'18"	106°29'19"	sandstone	Cretaceous	419(1375)	77.4	6.1	10.90	0.30	Lei et al., 2012
Borehole										
HB1-4	32°05'49"	107°06'07"	Sandstone	Jurassic	-68(-223)	73.1	4.7	12.48	0.20	Tian et al., 2011
HB1-5	32°05'49"	107°06'07"	Sandstone	Jurassic	-2594(-8510)	25.6	2.2	11.02	0.40	Tian et al., 2011
HB1-6	32°05'49"	107°06'07"	Sandstone	Jurassic	-2972(-9751)	16.1	1.5	10.62	0.34	Tian et al., 2011
HB1-8	32°05'49"	107°06'07"	Siltstone	Triassic	-3398(-11148)	17.3	3	10.00	0.45	Tian et al., 2011
HB1-9	32°05'49"	107°06'07"	Sandstone	Triassic	-3496(-11470)	14.0	2.5	11.15	0.41	Tian et al., 2011
HB1-1	32°05'49"	107°06'07"	Sandstone	Triassic	-4485(-14715)	8.8	1.3	10.22	0.48	Tian et al., 2011